Solid Earth

Tectonostratigraphic evolution of the Slyne Basin

Conor M. O'Sullivan[1,2,a], **Conrad J. Childs**[1,2], **Muhammad M. Saqab**[1,2,b], **John J. Walsh**[1,2], **and Patrick M. Shannon**[1,3]

[1]Irish Centre for Research in Applied Geoscience (iCRAG), O'Brien Centre for Science (East), University College Dublin, Belfield, Dublin 4, Ireland
[2]Fault Analysis Group, School of Earth Sciences, University College Dublin, Belfield, Dublin 4, Ireland
[3]School of Earth Sciences, University College Dublin, Belfield, Dublin 4, Ireland
[a]present address: Petroleum Experts, Petex House, 10 Logie Mill, Edinburgh, EH7 4HG, United Kingdom
[b]present address: Norwegian Geotechnical Institute, 40 St. Georges Terrace, Perth, WA 6000, Australia

**Correspondence:** Conor M. O'Sullivan (cmnosullivan@gmail.com)

Abstract. The Slyne Basin, located offshore NW Ireland, is a narrow and elongated basin composed of a series of interconnected grabens and half-grabens, separated by transfer zones coincident with deep crustal structures formed during the Silurian- to Devonian-aged Caledonian Orogeny. The basin is the product of a complex, polyphase structural evolution stretching from the Permian to the Miocene. Initially, relatively low-strain rifting occurred in the Late Permian and again in the latest Triassic to Middle Jurassic, followed by a third phase of high-strain rifting during the Late Jurassic. These extensional events were punctuated by periods of tectonic quiescence during the Early Triassic and Middle Jurassic. Late Jurassic strain was primarily accommodated by several kilometres of slip on the basin-bounding faults, which formed through the breaching of relay ramps between left-stepping fault segments developed during earlier Permian and Early–Middle Jurassic rift phases. Following the cessation of rifting at the end of the Jurassic, the area experienced kilometre-scale uplift and erosion during the Early Cretaceous and a second, less severe phase of denudation during the Palaeocene. These post-rift events formed distinct regional post-rift unconformities and resulted in a reduced post-rift sedimentary section. The structural evolution of the Slyne Basin was influenced by pre-existing Caledonian structures at a high angle to the basinal trend. The basin illustrates a rarely documented style of fault reactivation in which basin-bounding faults are oblique to the earlier structural trend, but the initial fault segments are parallel to this trend. The result is a reversal of the sense of stepping of the initial fault segments generally associated with basement control on basin-bounding faults.

1 Introduction

The north-western European Atlantic margin is made up of a framework of basins which are the product of a polyphase geological evolution stretching from Variscan orogenic collapse at the end of the Carboniferous to the formation of oceanic crust in the Eocene during the opening of the North Atlantic Ocean (Fig. 1a). The evolution of these basins is influenced by a variety of factors, including pre-existing faults and lineaments, typically inherited from the Caledonian or Variscan orogenies, and the presence of salt within the sedimentary basin fill, acting as layers of mechanical detachment. Caledonian and Variscan structures have been observed both reactivating and influencing the formation of younger structures during Late Paleozoic and Mesozoic rift events if oriented optimally (e.g. Stein, 1988; Schumacher, 2002; Wilson et al., 2010; Bird et al., 2014; Fazlikhani et al., 2017; Osagiede et al., 2020) or acting as barriers to fault growth and segmenting rift systems if they are oblique to the extension direction (e.g. Morley et al., 2004; Pereira and Alves, 2011, 2013; Phillips et al., 2018).

The Slyne Basin (250 km long and between 30 and 70 km wide) is a chain of grabens and half-grabens that occupy the eastern margin of the Rockall Basin (Fig. 1). The Slyne Basin shows significant along-strike structural variability, with changes in dip direction of the kilometre-scale basin-
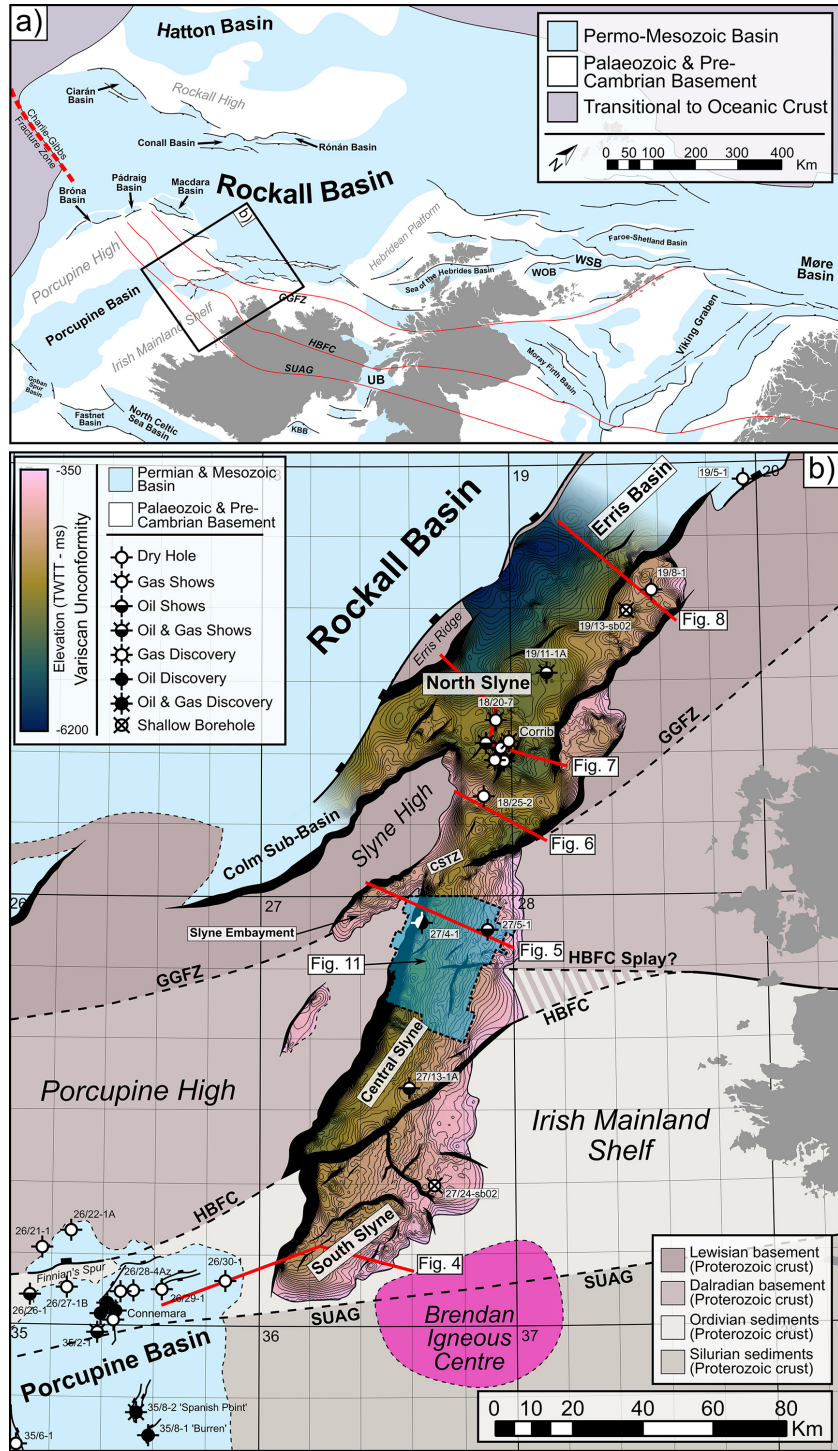
Figure 1. (a) Simplified structural map of the NW European Atlantic margin showing the study area in relation to other Permian and Mesozoic sedimentary basins, adapted from Doré et al. (1999) and Naylor et al. (1999). Caledonian structural lineaments which segment the basins are shown in red. Abbreviations: GGFZ, Great Glen Fault Zone; HBFC, Highland Boundary–Fair Head–Clew Bay Lineament; KBB, Kish Bank Basin; SUAG, Southern Uplands–Antrim–Galway Lineament; UB, Ulster Basin; WOB, West Orkney Basin; WSB, West Shetland Basin. **(b)** Time structure map of the Base Permian or Variscan Unconformity in the Slyne Basin. Local sub-basins and structural elements are labelled. Approximate location of Caledonian structures are highlighted outside the Slyne Basin with dashed black lines. Primary basement composition adapted from Štolfová and Shannon (2009). Abbreviations: CSTZ, Central Slyne Transfer Zone.

bounding faults occurring at transfer zones. The transfer zones are commonly observed where crustal-scale lineaments and terrane boundaries of Caledonian age transect the younger Late Palaeozoic and Mesozoic rifts. Similar phenomena have been observed in rift basins across the world, where pre-existing zones of weakness can influence the development of younger structures and where strain is transferred between them, i.e. the formation of transfer zones between large fault systems. The north-western European Atlantic margin is underlain by a series of pre-existing structures, and structural inheritance has been well documented in the Norwegian and UK Atlantic margins (Doré et al., 1999, 2007; Ady and Whittaker, 2019; Schiffer et al., 2019) as well as in the Iberian Atlantic margin (Alves et al., 2006; Pereira et al., 2017).

The structural geology of the Slyne Basin was the subject of significant study during the late 1990s and early 2000s following the discovery of the Corrib gas field in 1996 (Dancer et al., 2005). Previous publications documented aspects of the structural evolution (Chapman et al., 1999; Dancer et al., 1999) and the role of exhumation in the petroleum system of the basin (Corcoran and Doré, 2002; Corcoran and Mecklenburgh, 2005), as well placing the basin in the regional context of the Irish Atlantic margin (e.g. Corfield et al., 1999; Walsh et al., 1999). In recent years, significantly more and higher-quality seismic data, together with additional well data, have been acquired throughout the Slyne Basin and neighbouring areas (Shannon, 2018). Additionally, a comprehensive biostratigraphic study of all the Irish offshore basins has reclassified the ages of key syn-rift sequences (Merlin Energy Resources Consortium, 2020), warranting fresh investigation into the structural evolution of the Slyne Basin and its context within the greater Irish Atlantic margin.

This study utilises an extensive database of borehole-constrained 2D and 3D seismic reflection data, coupled with the results from the new biostratigraphic database, to investigate the structural evolution of the Slyne Basin. Key aspects of this structural history, including the development of the major basin-bounding faults, the role of salt in basin evolution, and influence of pre-existing crustal structures in the segmentation of the Slyne Basin, are examined and characterised. These findings are then placed in a regional context to better understand the role of the Slyne Basin in the evolution of the greater Irish Atlantic margin.

2 Geological setting

The Slyne Basin has a relatively flat present-day bathymetry, with water depths ranging from 100 to 600 m across most of the study area, with water depths increasing up to 2500 m in the north (Dancer et al., 1999). It is divided into three distinct sub-basins: the northern, central, and southern Slyne sub-basins (Fig. 1b; sensu Trueblood and Morton, 1991). These are separated by transfer zones (sensu Morley et al., 1990;

Gawthorpe and Hurst, 1993) which coincide with the location of major structural lineaments, in the form of Caledonian terrane boundaries. Three Caledonian structures are mapped in Fig. 1b.

The Slyne Basin is bounded along its eastern margin by the Irish Mainland Shelf, while the Porcupine and Slyne highs make up the western boundary (Fig. 1b). The Colm Basin, previously identified as a distinct Mesozoic basin (Dancer et al., 1999), appears to be an extension of the northern Slyne sub-basin, verging south-westwards between the Rockall Basin and the Porcupine High. A narrow, discontinuous basement horst which represents a southern extension of the Erris Ridge (Cunningham and Shannon, 1997) separates the northern Slyne sub-basin and the neighbouring Erris Basin from the Rockall Basin to the north-west. Similarly, a narrow basement high separates the southern Slyne sub-basin from the Porcupine Basin to the south-west.

2.1 Basement configuration

Previous authors have noted the role of pre-existing Caledonian structures in the segmentation of younger Mesozoic basins on the Irish Atlantic margin, correlating the offshore extension of these crustal-scale structures with complex transfer zones separating distinct sub-basins (Trueblood and Morton, 1991; Dancer et al., 1999). Several authors have mapped the offshore extent of Caledonian structural lineaments on the Irish Atlantic margin (Lefort and Max, 1984; Tate, 1992; Naylor and Shannon, 2005; Štolfová and Shannon, 2009; Kimbell et al., 2010). There are three Caledonian structures relevant to the evolution of the Slyne Basin: the Great Glen Fault Zone (GGFZ), the Highland Boundary–Fair Head–Clew Bay Fault Zone (HBFC), and the Southern Uplands–Antrim–Galway Fault Zone (SUAG; Fig. 1b). The exact locations of these structures in the vicinity of the Slyne Basin are variably constrained; the NE–SW-trending GGFZ has been mapped across the Irish Mainland Shelf to the west of the Erris Basin using deep seismic profiles and potential field datasets as a vertical strike-slip fault (Klemperer et al., 1991; Kimbell et al., 2010). The GGFZ intersects the Slyne Basin between the northern and central Slyne sub-basins at a location termed the Central Slyne Transfer Zone (CSTZ; sensu Dancer et al., 1999). The HBFC and SUAG structures are more poorly constrained; the HBFC is an E–W-oriented structure bounding the southern shore of Clew Bay on the west coast of Ireland and is mapped passing through Clare Island due west of Clew Bay (Fig. 1; Badley, 2001; Worthington and Walsh, 2011). The HBFC may correlate with the fault zone separating the central and southern Slyne sub-basins, but there is also evidence that splays of the HBFC may also be observed in the central Slyne sub-basin (Fig. 1b). The SUAG structure has been mapped trending E–W along the northern shore of Galway Bay (REF) and south of the Slyne Basin, through the Brendan Igneous Centre (Fig. 1). Unlike the near-vertical GGFZ, both the HBFC and SUAG struc-

tures are more shallowly dipping normal and reverse fault zones, although evidence of strike-slip movement is recorded along-strike onshore Ireland (Badley, 2001; Worthington and Walsh, 2011; Anderson et al., 2018).

The Caledonian lineaments separate different basement terranes which were assembled during the Caledonian Orogeny and have been extended from their known extents onshore Ireland and Scotland by several authors (e.g. Roberts et al., 1999; Tyrrell et al., 2007; Štolfová and Shannon, 2009). Limited pre-Carboniferous well penetrations in the Slyne Basin preclude the accurate mapping of these basement terranes, and the interpretations of previous authors are adopted here (Fig. 1b).

2.2 Stratigraphic framework of the Slyne Basin

Previous stratigraphic nomenclature for the Slyne Basin was largely based on comparisons with the geology of the Hebridean basins exposed on the Isle of Skye (e.g. Trueblood and Morton, 1991). An updated stratigraphic nomenclature with revised biostratigraphy has recently been published, standardising nomenclature at group, formation, and member levels across the sedimentary basins of the Irish Continental Shelf (Merlin Energy Resources Consortium, 2020). This stratigraphic nomenclature is used in this study (Fig. 2). The high-strain Middle Jurassic syn-rift section of previous authors (e.g. Chapman et al., 1999; Dancer et al., 1999; Corcoran and Mecklenburgh, 2005; Dancer et al., 2005) has recently been reclassified as Late Jurassic in age. This has important implications for regional geodynamics, which are discussed below. For full details on the biostratigraphic reclassification please refer to Merlin Energy Resources Consortium (2020).

The pre-rift section of the Slyne Basin consists of Carboniferous mudstones and sandstones with interbedded layers of coal, underlain by Silurian and older metasediments (Merlin Energy Resources Consortium, 2020). The Carboniferous sediments are overlain by an evaporite-rich Permian sequence, which is a lateral equivalent of the Zechstein Group encountered throughout NW Europe (O'Sullivan et al., 2021). The overlying Triassic section is sub-divided into Lower Triassic fluvial sandstones and Upper Triassic playa; sabkha and lacustrine mudstones; and claystones interbedded with thin limestone, sandstone, and anhydrite beds (Dancer et al., 2005; Štolfová and Shannon, 2009). A massive halite unit is present at the base of the Upper Triassic section in the northern Slyne sub-basin but is absent in the central and southern parts of the basin (O'Sullivan et al., 2021).

The Lower Jurassic section is composed of marine sandstone, mudstones, and carbonates, overlain by Middle Jurassic calcareous marine mudstones (Trueblood and Morton, 1991; Dancer et al., 1999). The Kingfisher Limestone Member is a unit of thick limestones that occurs at the base of Kestrel Formation (sensu Merlin Energy Resources Consortium, 2020) and which forms a distinct, semi-regional seismic marker termed the "Bajocian Limestone Marker" in previous literature (e.g. Trueblood and Morton, 1991; Scotchman and Thomas, 1995; Dancer et al., 1999). A regional unconformity separates the underlying Lower and Middle Jurassic sections from the overlying Upper Jurassic sediments. The Upper Jurassic section consists of terrestrial and fluvio-estuarine mudstones and sandstones with numerous palaeosols and coal layers, which are overlain by the marine mudstones, indicating that a regional marine transgression occurred during the late Oxfordian to Tithonian (Merlin Energy Resources Consortium, 2020).

The Base Cretaceous Unconformity separates the Cretaceous section of the Slyne Basin from the underlying Jurassic strata. The Lower Cretaceous stratigraphy consists of Albian-aged glauconitic mudstones and sandstones, while the overlying Upper Cretaceous section is composed of limestones and calcareous mudstones. The Base Cenozoic Unconformity forms the lower boundary to the Cenozoic succession in the Slyne Basin. The Cenozoic section can be subdivided into three sequences: a layer of Eocene lava locally developed in the northern and southern areas of the Slyne Basin; overlain by an Eocene–Miocene section and a Miocene to Quaternary section, both consisting of poorly consolidated marine mudstones and sandstones; separated by a mid-Miocene unconformity.

3 Dataset and methodology

This study focused on the interpretation of an extensive suite of multi-vintage 2D and 3D seismic reflection data collected during hydrocarbon exploration in the Slyne Basin (Fig. 3). The 2D seismic dataset consists of 17 surveys acquired between 1980 and 2007, comprising over 22 000 line-kilometres of data, while the 3D seismic dataset consists of eight surveys acquired between 1997 and 2013 and covers almost 4000 km^2. Seismic data quality varies from very poor to good, with the more modern vintages typically providing clearer imaging. Data quality in the Slyne Basin is heavily influenced by the near-seabed geology, with the distribution of Cenozoic lava flows and intrusive sills, coupled with Cretaceous chalk, causing imaging problems including multiples, energy scattering, and signal attenuation (Dancer and Pillar, 2001). These problems are most severe in the northern Slyne sub-basin and the western margin of the southern Slyne sub-basin. The application of modern processing techniques and use of 3D seismic data have improved data quality in the region somewhat (Dancer and Pillar, 2001; Droujinine et al., 2005; Rohrman, 2007; Hardy et al., 2010), most recently with the acquisition of an ocean-bottom cable survey over the Corrib gas field in 2012 and 2013 (Shannon, 2018). Seismic sections are presented in European polarity (Brown, 2001), where a positive downwards increase in acoustic impedance corresponds to a positive (red) reflection event, and a decrease corresponds to a negative (blue) reflection event. All
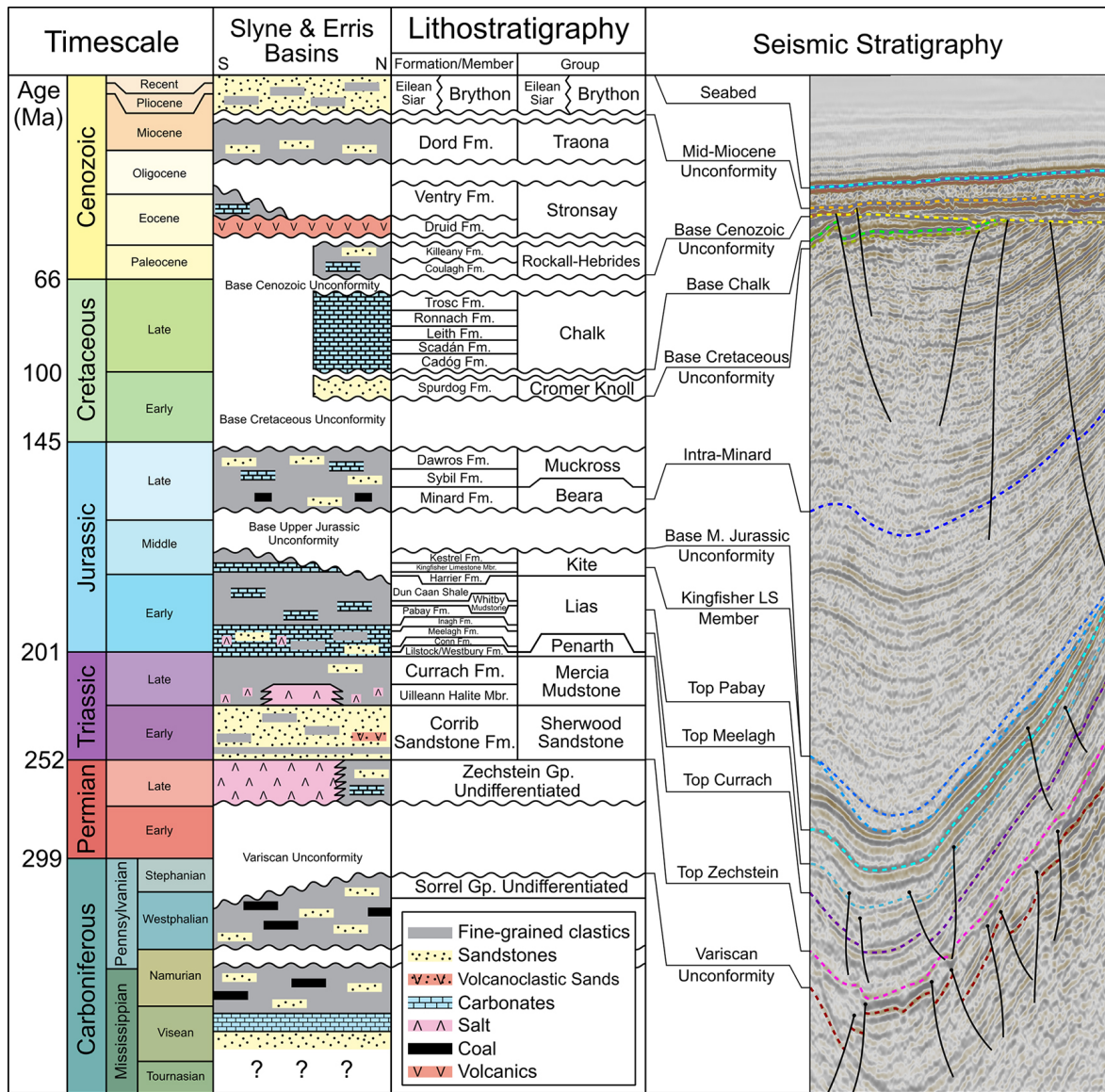
Figure 2. Lithostratigraphic chart showing the simplified stratigraphy of the Slyne Basin, age of key horizons, and typical seismic stratigraphy from the central Slyne sub-basin. Stratigraphic column adapted from Merlin Energy Resources Consortium (2020).

sections are vertically exaggerated by a factor of 3, and ball ends are used to highlight where a fault terminates within a certain stratigraphic package, while faults without ball ends are truncated by a younger unconformity.

Thirteen key horizons were mapped across the Slyne Basin in the time domain (Fig. 2). The ages of these horizons were constrained using exploration and appraisal wells in addition to shallow boreholes. The northern Slyne sub-basin has the highest well density, including eight appraisal and production wells associated with the Corrib gas field and four near-field exploration wells (19/8-1, 19/11-1A, 18/20-7, and 18/25-2), with a further three exploration wells in the central Slyne sub-basin (27/4-1, 27/5-1, and 27/13-1). The stratigraphy of the southern Slyne sub-basin is uncon-

strained except for a single shallow borehole (27/24-sb02A), which proved Lower Jurassic and Upper Triassic sediments beneath the Base Cenozoic Unconformity (Fugro, 1994a). The dataset associated with the exploration, appraisal, and production wells consists of comprehensive suites of wireline logs (gamma, caliper, neutron-density, sonic, and resistivity logs), well completion reports with formation tops, and time–depth relationship data as either checkshots or vertical seismic profiles (VSPs).
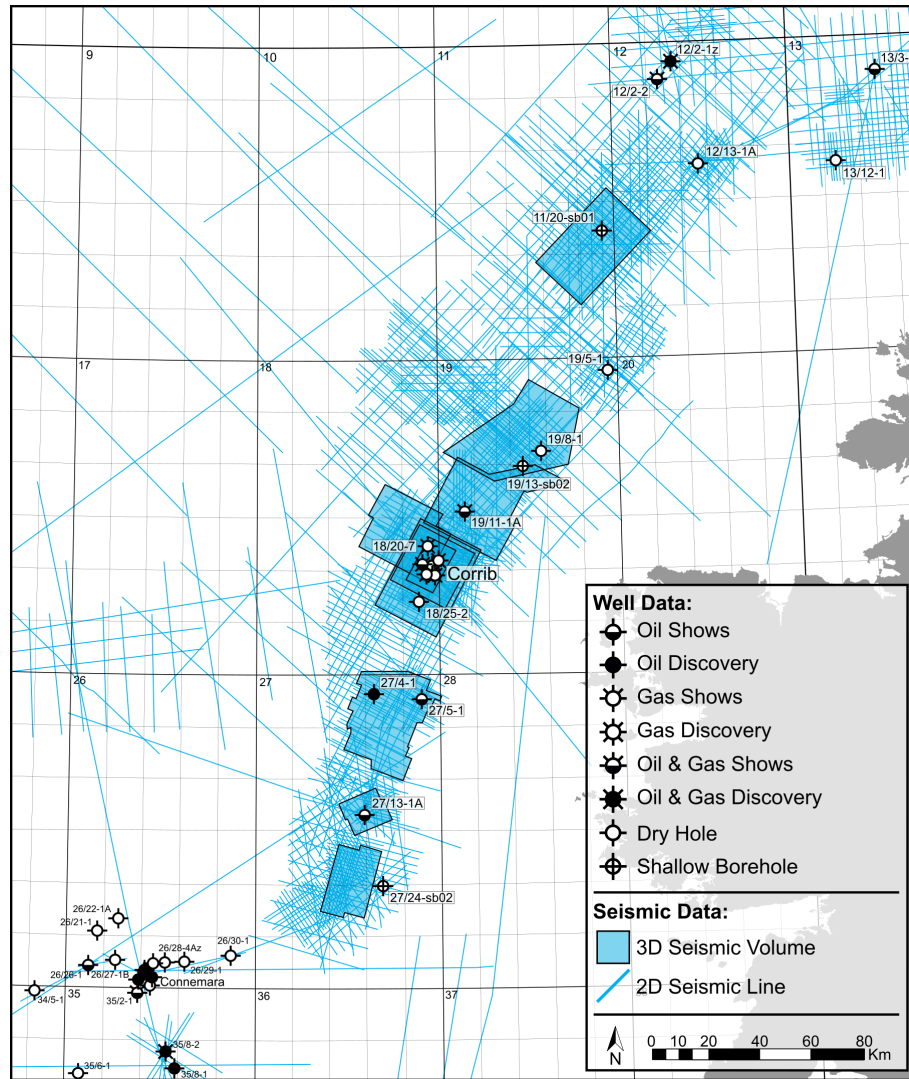
**Figure 3.** Map showing study area and datasets used.

4 Results

4.1 Basin geometry and transfer zones

The southern and central Slyne sub-basins are half-grabens which dip towards the north-west (Figs. 4 and 5), with a NNE–SSW-oriented basin-bounding fault separating them from the Porcupine High to the west. As no Permian or Mesozoic strata are preserved on the footwall of these basin-bounding faults (the Porcupine High) either through non-deposition or erosion (Figs. 4 and 5), the total throw on these faults is difficult to constrain. Nevertheless, the elevation of the Base Permian Unconformity in the adjacent hanging wall provides a minimum throw estimate of 3000 ms TWTT (two-way travel time) along most of the length of this fault (Fig. 1b). Unlike its southern and central neighbours, the northern Slyne sub-basin is an eastward-dipping graben

(Figs. 6 and 7) bounded by a series of segmented faults along its eastern boundary with the Irish Mainland Shelf (Fig. 1b), while a narrow basement horst separates it from the Rockall Basin to the north-west. The fault system bounding the eastern margin of the northern Slyne sub-basin consists of a series of left-stepping, NE–SW-oriented faults linked by relay ramps (Fig. 1b). These faults are of a similar scale to the fault bounding the southern and central Slyne sub-basins, with over 3000 ms TWTT of throw recorded (Fig. 1b). The northernmost segment of this fault system separates the Slyne Basin from the Erris Basin to the north, with the Erris Basin being downthrown relative to the northern Slyne sub-basin across this fault (Fig. 8).

The reversal of basin polarity occurs across the CSTZ, which coincides with the intersection of the offshore extension of the GGFZ and the Slyne Basin (Fig. 1b). Deep seismic transects adjacent to the Slyne Basin image the GGFZ
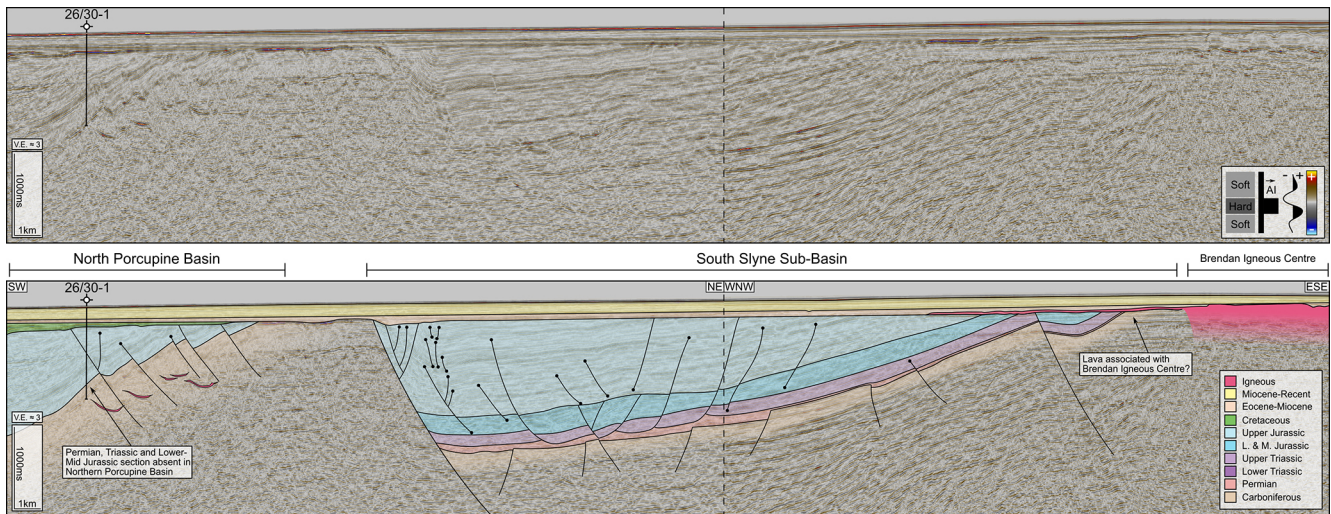
Figure 4. Composite section of 2D seismic lines NWI-93-202 and NWI-93-028 and accompanying geoseismic interpretation covering the southern Slyne sub-basin, North Porcupine Basin, and Brendan Igneous Centre. The southern Slyne sub-basin is a westward-dipping half-graben and is downthrown relative to the North Porcupine Basin, separated by a narrow high composed of crystalline basement. See Fig. 1 for location.
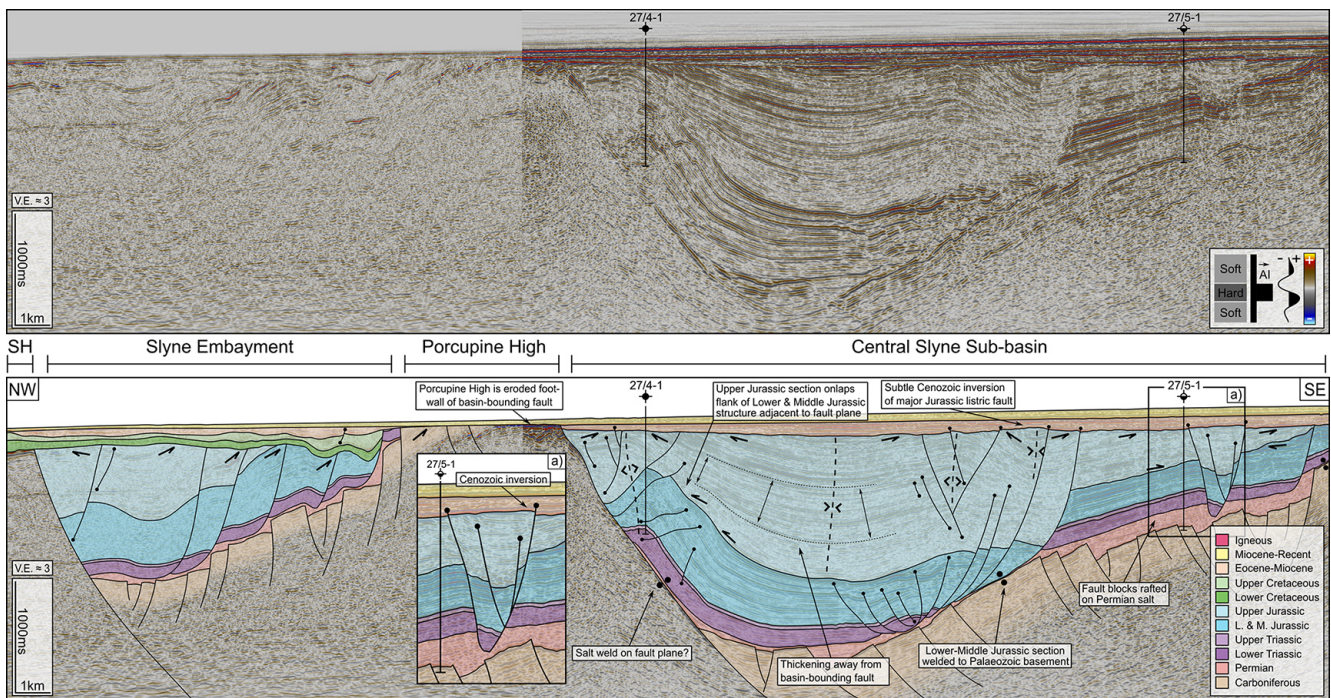
Figure 5. Composite seismic section of 2D seismic line E96IE09-28 and inline 2740 from the 2000/2008 (E00IE09) 3D seismic volume from the central Slyne sub-basin, with accompanying seismic interpretation. See Fig. 1 for location. Abbreviations: PH, Porcupine High.

as a NE–SW-trending vertical discontinuity which appears to offset the Moho (Klemperer et al., 1991). The throw on the basin-bounding faults north and south of the CSTZ rapidly decreases as they approach the CSTZ so that horizons are continuous between the basins, and strain is transferred between the faults of opposed polarity via a convergent, con-jugate transfer zone (sensu Morley et al., 1990). Both faults have over 3000 ms TWTT of throw on the Base Permian Unconformity within 10 km of the CSTZ (Figs. 1, 5, 6), with this value likely being an underrepresentation of the true throw given the kilometre-scale erosion of Jurassic sediments recorded both north and south of the CSTZ beneath the post-
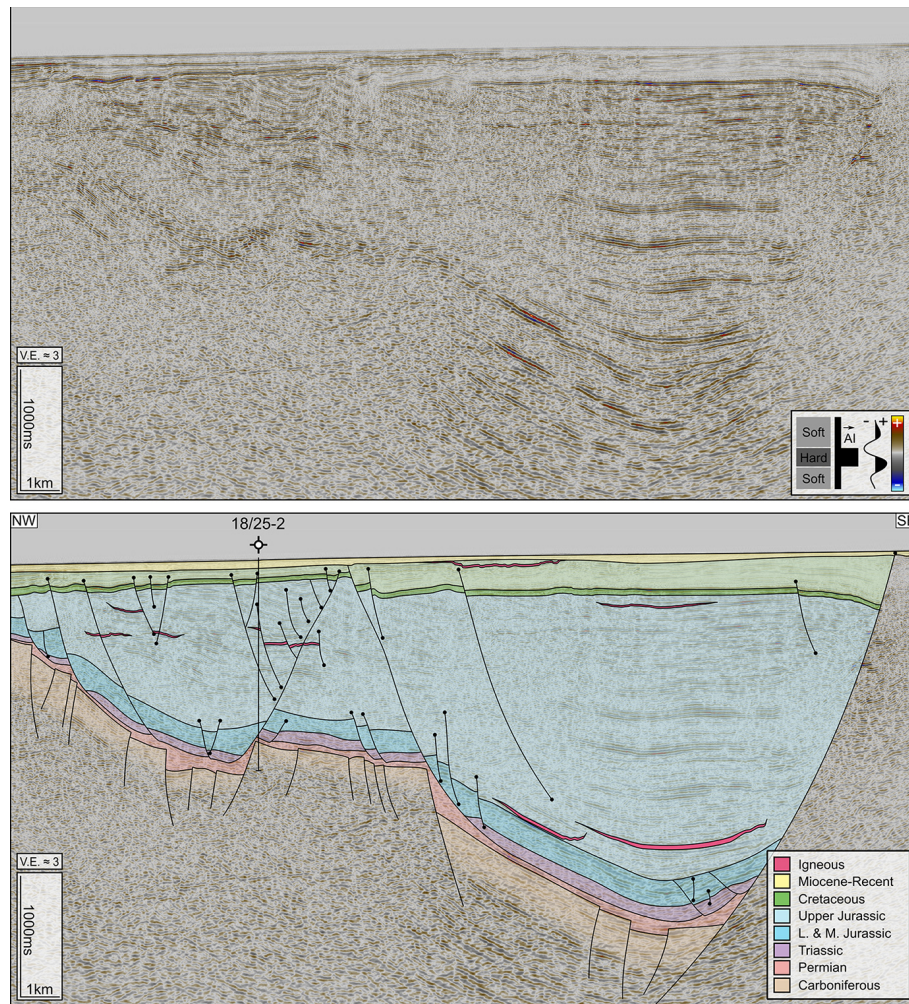
Figure 6. The 2D seismic line E93IE07 and accompanying geoseismic interpretation from the Central Slyne Transfer Zone. Basin polarity has switched from the westward-dipping half-graben geometry of the central and southern Slyne sub-basins to an eastward-dipping half-graben geometry. The presence of near-seabed Upper Cretaceous Chalk causes a significant reduction in image quality. See Fig. 1 for location.

rift unconformities (e.g. Corcoran and Mecklenburgh, 2005; Biancotto et al., 2007). In addition to the faults bounding the central and northern Slyne sub-basins, a NE–SW-oriented, southward-dipping fault bounds the Slyne Embayment, a small half-graben to the south-west of the CSTZ (Figs. 1b, 5). This suggests that the GGFZ localised the formation of the transfer zone between the basin-bounding faults to the north and south. Pre-existing deformation in the Caledonian-aged basement associated with the structure likely formed a preferential zone to transfer strain between the younger Permo-Mesozoic faults during these extensional episodes.

The HBFC fault is interpreted as a hard-linked NE–SW-oriented fault, dipping towards the NW, which downthrows the central Slyne sub-basin relative to the southern Slyne sub-basin (Fig. 1b). The HBFC fault also appears to offset the NNE–SSW-oriented fault bounding the central and southern Slyne sub-basins with a sinistral sense of motion (Fig. 1b). This map-view shape may be a product of both normal dip-

slip movement, preserving more of the syn-rift basin beneath the post-rift unconformity in the hanging wall of the HBFC fault, and sinistral strike-slip movement recorded onshore Ireland (e.g. Worthington and Walsh, 2011; Anderson et al., 2018). The nature of the interaction between these two faults is unclear due to poor seismic image quality caused by shallow Cenozoic lavas which blanket the western margin of the southern Slyne sub-basin. However, the lateral offset of the NE–SW-oriented basin-bounding fault and the adjacent Porcupine High either side of the HBFC fault is well imaged on seismic sections immediately north and south of this zone.

4.2 The role of salt in basin development

The Slyne Basin contains two layers of salt: the Permian Zechstein Group and the Upper Triassic Uilleann Halite Member (Fig. 9a; Dancer et al., 2005; Merlin Energy Resources Consortium, 2020). The Zechstein Group is com-
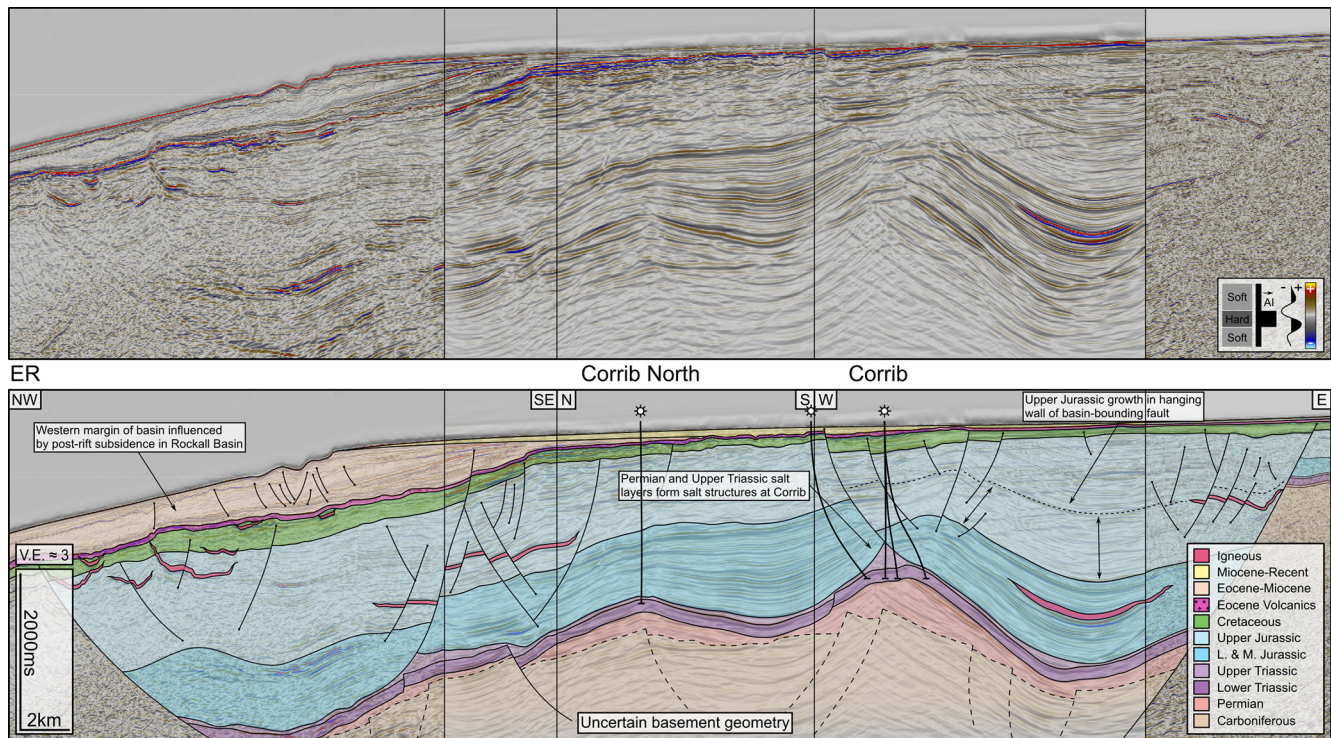
Figure 7. Composite section of an arbitrary line from the Iniskea 2018 3D volume and 2D seismic line ST9808-1002 from the northern Slyne sub-basin and accompanying geoseismic interpretation. Significantly thicker Zechstein salt in this part of the Slyne Basin forms salt pillows and salt anticlines, folding the overlying Mesozoic section. Detachment on the Uilleann Halite causes rafting and listric faulting in the overlying Jurassic section. See Fig. 1 for location. Abbreviations: ER, Erris Ridge.

posed of both halite and anhydrite, while the Uilleann Halite Member is composed predominantly of halite interbedded with red mudstone and anhydrite (O'Sullivan et al., 2021).

In the central and southern Slyne sub-basins, south of the CSTZ, only the Zechstein Group salt is present (Fig. 2), where it mechanically detaches the sub-salt basement from the Mesozoic supra-salt basin fill (Figs. 4–5, 9, 10). Several halokinetic structures are present in the central and southern Slyne sub-basins, including large salt rollers, collapsed diapirs, and rafted fault blocks (Figs. 5, 9). There are also several high-relief monoclines adjacent to the basin-bounding fault in the central Slyne sub-basin which have been noted by previous authors (Fig. 5; Dancer et al., 1999). The Triassic and Lower–Middle Jurassic section in these structures is encountered at a similar depth to the same section along the eastern margin of the basin, and the Triassic section appears to have welded to the crystalline basement of the Porcupine High across the fault plane of the basin-bounding fault (Fig. 5). These structures likely formed initially as forced folds above the sub-salt basin-bounding faults during the early stages of rifting in the Late Jurassic, resulting in the Upper Jurassic section onlapping the flank of these structures. As extension continued, the fault breached the salt and led to the present geometry (O'Sullivan et al., 2021).

In the northern Slyne sub-basin both the Permian and Upper Triassic salt layers are present (Fig. 9a; Corcoran and Mecklenburgh, 2005; O'Sullivan et al., 2021). Here, both layers mechanically detach the stratigraphy above and below them, with the Permian salt detaching the Lower Triassic from the carboniferous basement, while the Upper Triassic salt detaches the Jurassic section from the Lower Triassic (Figs. 7, 9b). Halokinetic structures formed in the Permian and Triassic salts are often coincident and can be demonstrated to be kinematically related. This is exemplified by the structure containing the Corrib gas field (Figs. 7, 9; Corcoran and Mecklenburgh, 2005; Dancer et al., 2005); here, the Permian salt forms a NE–SW-trending salt pillow, which folds the overlying Mesozoic sediments. An Upper Triassic salt wall formed parallel to the fold axis of the Permian salt pillow and forms the footwall to a listric fault which downthrows the folded Jurassic section to the SE (Figs. 7, 9b). The evolution of the structure hosting the Corrib gas field is discussed in detail in O'Sullivan and Childs (2021).

Several of the halokinetic structures in the Slyne Basin record several discrete periods of growth and development. There is significant evidence for halokinesis during the Early and Middle Jurassic, with the crests of fault blocks cored by salt rollers eroded by the Base Upper Jurassic Unconformity (e.g. Fig. 9c–d). There is also evidence for Per-
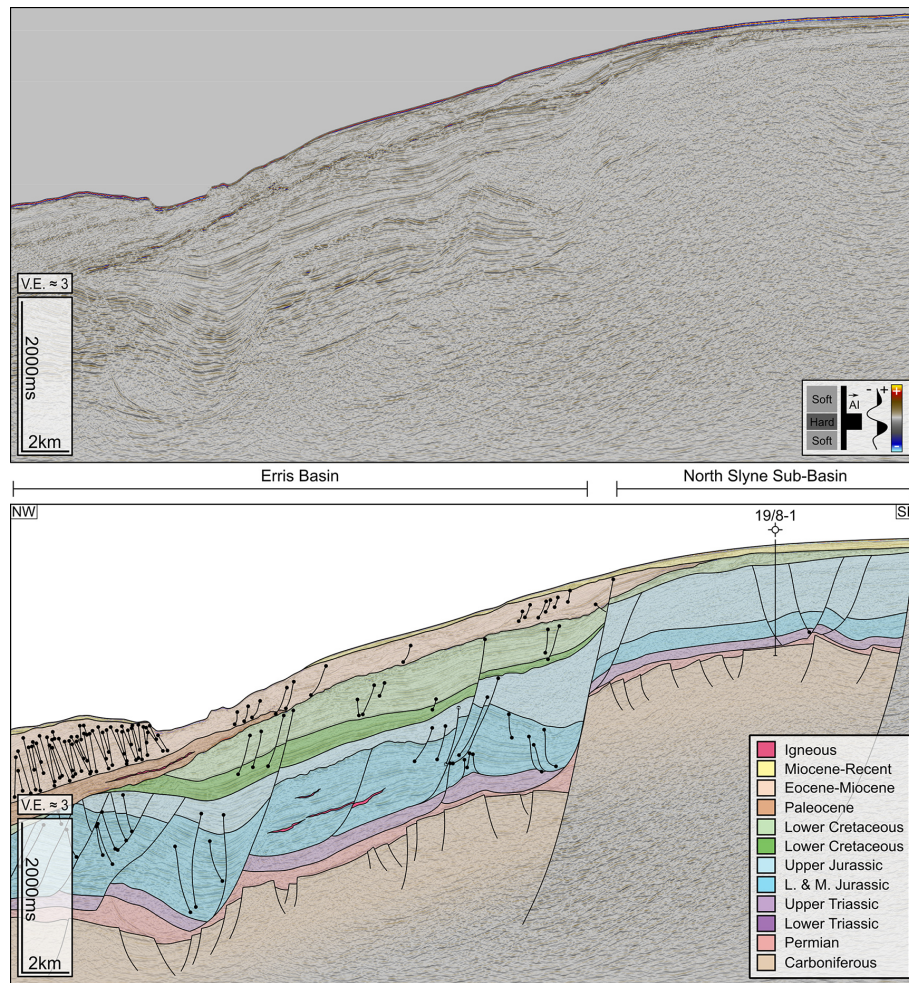
Figure 8. The 2D seismic line ST9505-430 and accompanying geoseismic interpretation covering the northern Slyne sub-basin and the southern Erris Basin. The Erris Basin is downthrown relative to the Slyne Basin and has a significantly thicker Lower and Middle Jurassic section preserved but conversely reduced Upper Jurassic stratigraphy. Significantly thicker Cretaceous and Cenozoic post-rift stratigraphy is preserved in the Erris Basin relative to the Slyne Basin. See Fig. 1 for seismic line location.

mian salt diapirs forming in the central Slyne sub-basin during the Early to Middle Jurassic which collapsed during the Late Jurassic extensional episode, as recorded in the reduced Lower and Middle Jurassic section observed in narrow fault-bounded grabens (e.g. Fig. 9c; Vendeville and Jackson, 1992; O'Sullivan et al., 2021). Several other halokinetic structures were also reactivated during Late Jurassic extension, including the structure containing the Corrib gas field, with significant Late Jurassic throw recorded on the listric fault above the Triassic salt wall (Fig. 9b). Some of these salt structures have also undergone minor modification during the Cretaceous and Cenozoic. Post-rift modification of salt structures was relatively minor compared to deformation associated with the Upper Jurassic phase of rifting, with offsets of ca. 10–100 ms TWTT observed on post-rift surfaces (e.g. Figs. 5, 9c). Some of the salt-related post-rift fault movement is observed on the listric fault above the Corrib structure with

a distinct Cretaceous growth sequence recorded in the hanging wall of this fault (Fig. 9b).

4.3 Structural evolution of the Slyne Basin

The observations of basin geometry and salt tectonics presented above are now combined with further structural analysis to understand the evolution of the Slyne Basin. This section is divided into sections which broadly correlate with the main tectonic phases observed in the basin, with three episodes of syn-rift extension in the Permian, Early–Middle Jurassic, and Late Jurassic followed by post-rift modification during the Cretaceous and Cenozoic.

4.3.1 Permian and Triassic

Post-Variscan extension began in the Slyne Basin during the Late Permian. Several hundred metres of Zechstein halite
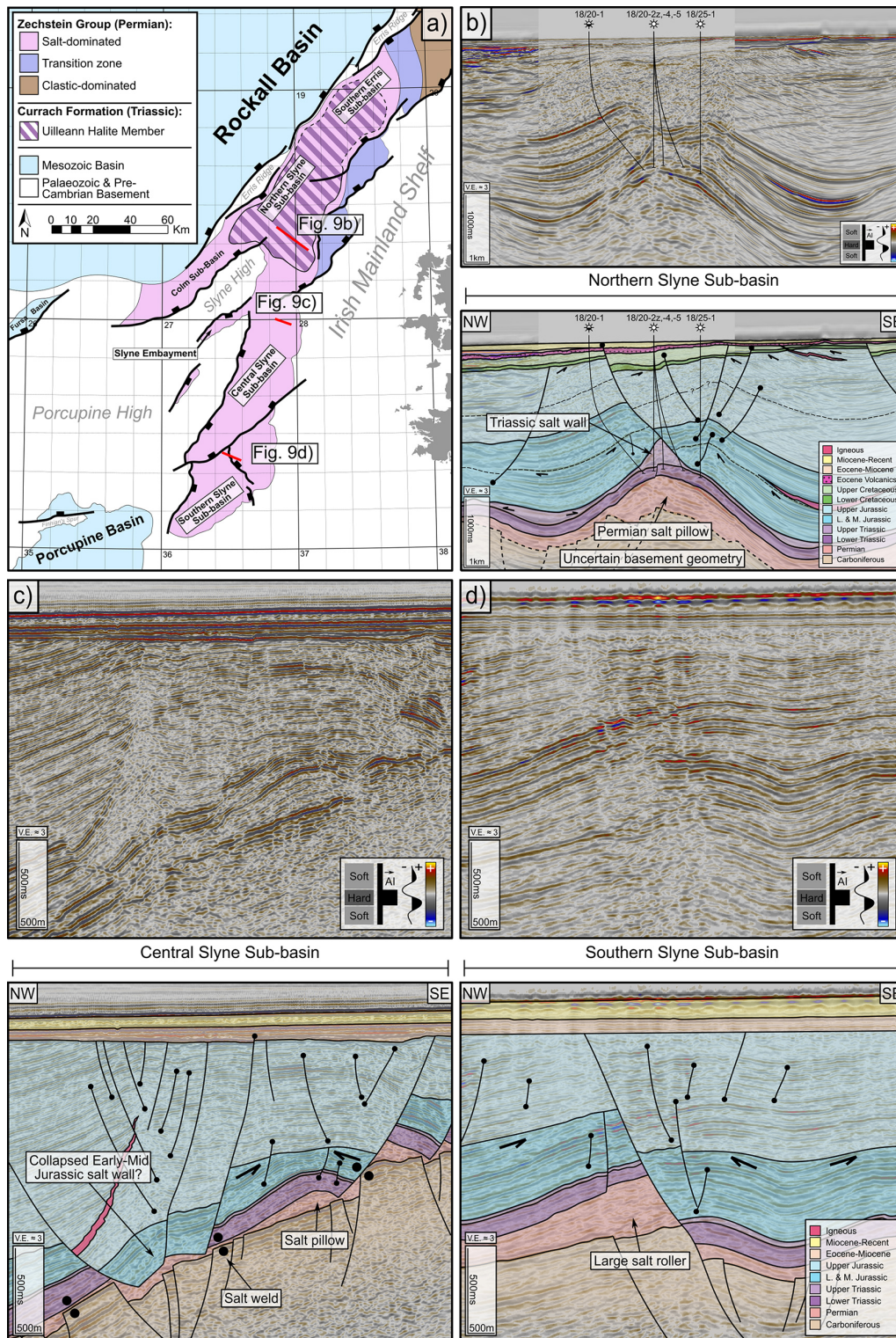
Figure 9. Seismic sections and accompany interpretations showing salt structures in the Slyne Basin. **(a)** Map showing the distribution of Upper Triassic and Permian salt in the Slyne Basin. Adapted from O'Sullivan et al. (2021). **(b)** Seismic and geoseismic section through the Corrib gas field showing the kinematic interaction between Upper Triassic and Permian salt. The Permian salt forms a NE–SW-oriented salt pillow, while the Upper Triassic forms an elongated salt wall parallel to the fold axis of the salt pillow. Adapted from O'Sullivan and Childs (2021). **(c)** Several salt-related structures in the central Slyne sub-basin, including a salt pillow, salt roller, and an apparent collapsed salt diapir. **(d)** A large salt roller from the southern Slyne sub-basin. The fault in the supra-salt section appears to have hard-linked with the sub-salt basement fault.

was deposited throughout the Slyne Basin (Fig. 9a), likely in fault-bounded depocentres (O'Sullivan et al., 2021). The Permian boundaries of the Slyne Basin are poorly understood due to post-Permian halokinesis, but it is clear that the Slyne Basin was an area of active extension, relative to the neighbouring Erris and Porcupine basins, with a thin (tens of metres thick) layer of predominately clastic and carbonate facies developed in the former (Robeson et al., 1988; O'Sullivan et al., 2021) and no evidence of Permian sediments in the latter (Jones and Underhill, 2011; Bulois et al., 2018).

The Triassic was a period of relative quiescence in the Slyne Basin, typified by the near-isopachous nature of the Lower Triassic section throughout the basin (Figs. 5, 7, 9). The local thickening of the Upper Triassic section in the synclines flanking the Corrib anticline (Figs. 7, 9b) suggests that low-strain extension may have begun during the Late Triassic, at least in the northern Slyne sub-basin (O'Sullivan and Childs, 2021).

4.3.2 Early and Middle Jurassic

Low-strain regional extension occurred throughout the Slyne Basin during the Early and Middle Jurassic. In the northern Slyne sub-basin, a comparison of the stratigraphic section encountered in basinward wells with the single available well located on the footwall of the basin-bounding faults demonstrates the growth in the Lower and Middle Jurassic section during this period of regional extension (Fig. 10). In the central Slyne sub-basin the Lower and Middle Jurassic section can be observed thickening towards the basin-bounding faults by a few tens of milliseconds TWTT (10–100 m; Fig. 11d), but this shape is accentuated by erosion of this section at the Base Upper Jurassic Unconformity on the basin margins (e.g. well 27/5-1 location in Fig. 5). The Lower and Middle Jurassic section is also observed thickening into the synclines flanking the salt-cored folds in the northern Slyne sub-basin (Figs. 7, 9b), indicating that the Permian salt was undergoing halokinesis during this period (O'Sullivan and Childs, 2021). There is also evidence of salt walls forming in the central Slyne sub-basin during the Early to Middle Jurassic along with large salt rollers beneath active listric faults soling out in the Permian Zechstein Group (Figs. 9c, d, 11d).

A regional unconformity separates the Lower to Middle Jurassic from the Upper Jurassic section throughout the Slyne Basin, termed the Base Upper Jurassic Unconformity. This unconformity can be quite rugose on the margins of the basins, such as the area around the 27/5-1 well in the central Slyne sub-basin (Fig. 5), while being a relatively flat paraconformity in the centre of the basin (e.g. Figs. 5, 7). There are several angular truncations observed throughout the Slyne Basin at the base of this unconformity, particularly above salt-related structures formed during Early to Middle Jurassic extension, including footwalls above salt rollers and the crests of folds above salt pillows (Fig. 9c, d).

Throughout the Slyne Basin the late Middle Jurassic (Bathonian and Callovian) section is absent at this unconformity, either through erosion or non-deposition (Merlin Energy Resources Consortium, 2020). The exact cause of this unconformity is difficult to constrain, although some authors have suggested thermal doming and dynamic topography above a mantle plume similar to that implicated in the North Sea (Tate and Dobson, 1989; Underhill and Partington, 1993; Doré et al., 1999).

4.3.3 Late Jurassic

The main phase of extension commenced during the Late Jurassic, with the basin-bounding faults accumulating several kilometres of throw during this extensional episode along with the deposition of several kilometres of Upper Jurassic sediment (Figs. 4–8). Despite this, there are no obvious growth sequences observed in the southern Slyne sub-basin (Fig. 4) or in the southern portion of the northern Slyne sub-basin (Fig. 6). Growth sequences are observed in the hanging walls of the bounding faults in the northern Slyne sub-basin with reflectors diverging towards the SE (Fig. 7). In the central Slyne sub-basin, the Upper Jurassic section onlaps the flank of the high-relief monocline in the immediate hanging wall of the basin-bounding fault and thickens into the hanging wall of major intra-basinal listric fault (Fig. 5). This stratal geometry, along with a similar thickness of Lower–Middle Jurassic sediment present in the neighbouring Slyne Embayment, suggests that most of the slip on the fault bounding the central Slyne sub-basin accumulated during the Late Jurassic, with the kilometre-scale post-rift uplift and erosion during the Cretaceous and Cenozoic removing any Jurassic sediment from the intervening footwall, forming the Slyne High (Fig. 5). The presence of NE–SW-oriented fault splays in the sub-salt hanging wall of this fault (e.g. Fig. 11a) suggests that the large NNE–SSW-oriented fault bounding the central and southern Slyne sub-basins formed through the linkage of NE–SW-oriented fault segments, likely during this Late Jurassic phase of rifting.

Two discrete phases of Late Jurassic extension have been identified in the neighbouring Porcupine Basin, the first occurring in the Oxfordian and the second in the Kimmeridgian (Saqab et al., 2020). Both of these extensional episodes may have also occurred in the Slyne Basin, but, unlike the Porcupine Basin, a significant section of the Late Jurassic syn-rift section was subsequently removed during post-rift uplift and erosion (e.g. Corcoran and Mecklenburgh, 2005), and evidence of a second phase may have been removed. This may explain the lack of distinct growth sequences observed in the Upper Jurassic in the southern Slyne sub-basin, where movement on the bounding fault may have been matched by the sedimentation rate during the Oxfordian, followed by further movement occurring during the Kimmeridgian.
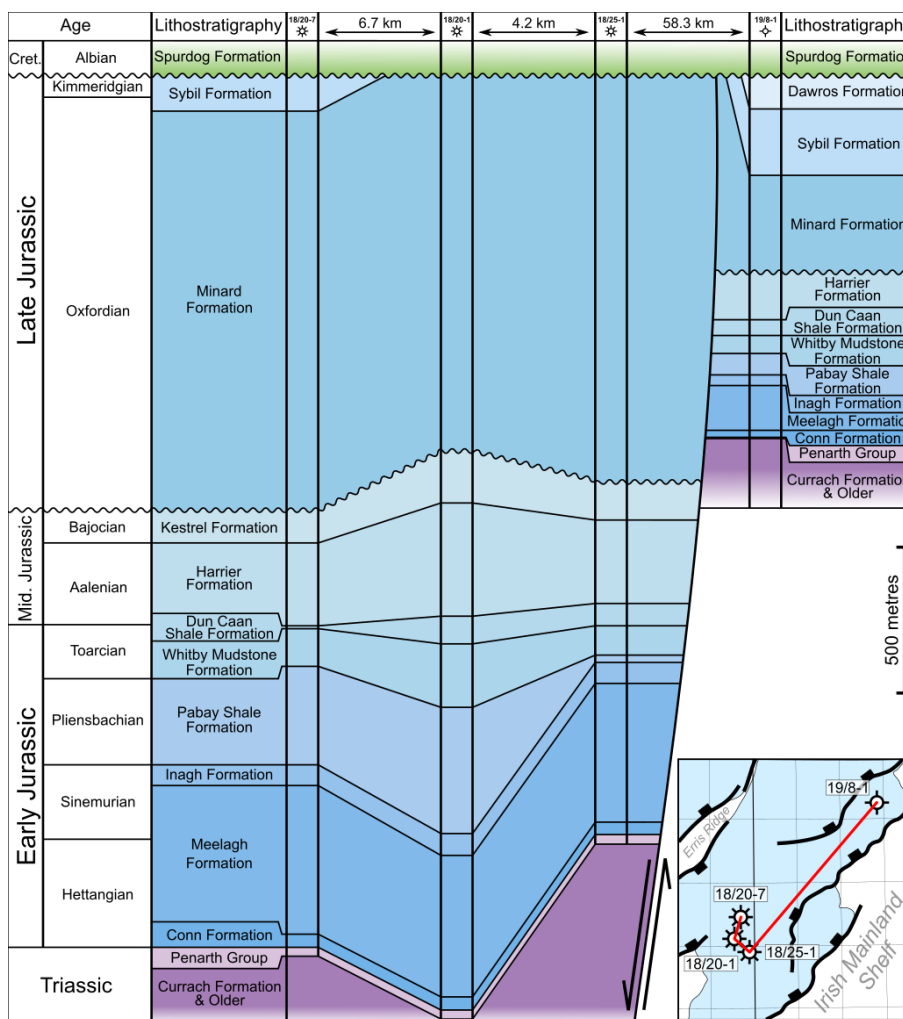
Figure 10. Well correlation through the Jurassic section of key wells from the northern Slyne sub-basin, highlighting thickness variations in the Lower and Middle Jurassic section between wells within the basin and the 19/8-1 well on the footwall of the basin-bounding fault system.

4.3.4 Cretaceous and Cenozoic

The Slyne Basin experienced kilometre-scale uplift and erosion at the end of the Jurassic and during the Early Cretaceous, removing a significant section of the Upper Jurassic syn-rift section throughout the basin (Table 1). The majority of the Slyne Basin was likely a topographic high relative to surrounding regions during the Cretaceous, including the Erris, Porcupine, and Rockall basins (Fig. 8; Musgrove and Mitchener, 1996; Chapman et al., 1999; Saqab et al., 2020). Up to 400 m of Albian and Late Cretaceous sediments was deposited in the northern Slyne sub-basin and the Slyne Embayment (Figs. 5–8, 12b) and possibly in the central and southern Slyne sub-basins. Several faults active during the Late Jurassic syn-rift phase were reactivated during the Cretaceous, with both normal and reverse movement observed throughout the Slyne Basin. In the northern Slyne sub-basin the listric fault above the Corrib anticline has a significant Cretaceous growth sequence that thickens from 200 ms TWTT (ca. 150 m) in the footwall to over 400 ms TWTT (ca. 380 m) in the hanging wall (Figs. 7, 9b). Additionally, the individual segments of the basin-bounding fault system along the eastern margin of the northern Slyne sub-basin were reactivated during the Cretaceous (Fig. 12b). The throw on the northern segment varies from 30–100 ms TWTT adjacent to the Corrib gas field through to the 19/8-1 well (Figs. 7, 8), while on the segment to the south, adjacent to the 18/25-2 well (Fig. 6), the throw locally exceeds 300 ms TWTT. In addition to these major faults, several smaller faults offset the Cretaceous section throughout the northern Slyne sub-basin, with the majority of these structures having throws less than 100 ms TWTT (Figs. 6, 7). The fault bounding the Slyne Embayment appears not to have been active during this time, with Cretaceous sediments overstepping the fault with no offset (Fig. 5). The absence of Cretaceous sediments in the central and southern Slyne sub-basins obscures
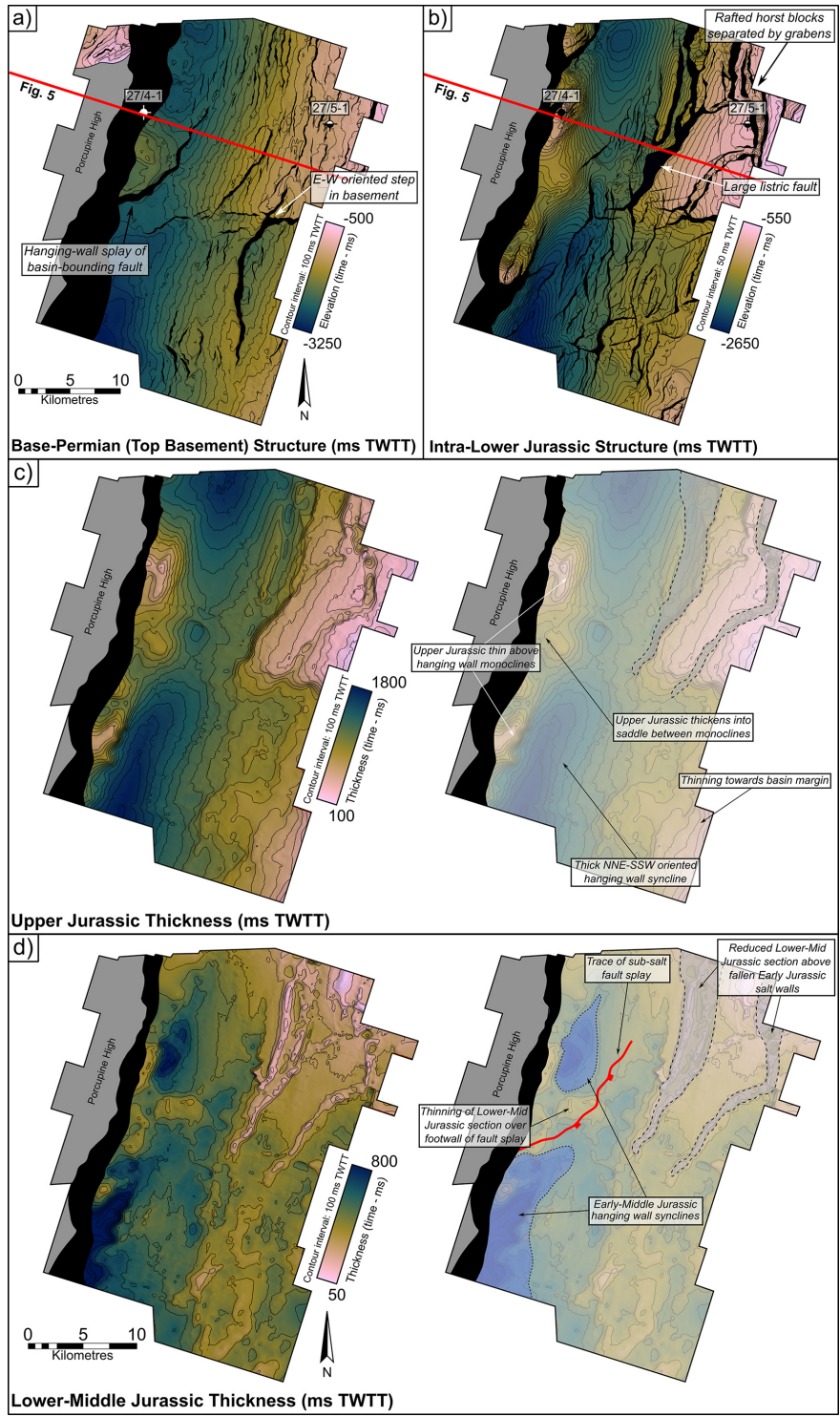
Figure 11. Structure and thickness maps (ms TWTT) from the E00IE09 3D seismic volume from the central Slyne sub-basin. See Fig. 1 for location. **(a)** TWTT structure map of the Variscan Unconformity. **(b)** TWTT structure map of the Top Meelagh Formation (intra-Lower Jurassic). Several high-relief anticlinal closures are present in the immediate hanging wall of the basin-bounding fault, including the structure containing the 27/4-1 "Bandon" oil accumulation. Note the significant differences in fault pattern between the Variscan Unconformity (pre-salt) and Top Meelagh Formation (post-salt). **(c)** TWTT thickness map of the Upper Jurassic. Note the thinning of the Upper Jurassic section onto the hanging-wall monoclines, including the structure drilled by the 27/4-1 well. **(d)** TWTT thickness map of the Lower and Middle Jurassic. Note the local thickening in the hanging wall of the fault splay in the sub-salt basement and the thinning in the north-east of the surface. This thinning is evidence of Zechstein salt diapirs which were present in the Early–Middle Jurassic, which then collapsed during Late Jurassic extension.

any fault activity that may have occurred during this period (Fig. 12b). Nevertheless, due to the pervasive nature of Cretaceous faulting in the northern Slyne sub-basin and strong evidence of Cretaceous faulting in the Porcupine Basin to the south-west (Jones and Underhill, 2011; Saqab et al., 2020), it is likely that some structures in the central and southern Slyne sub-basins were active during the Cretaceous. The motion on these faults would likely have been less than 100 ms TWTT, in a similar manner to those in the northern Slyne sub-basin. Alongside the reactivation of Late Jurassic syn-rift faults, the majority of which were oriented NNE–SSW parallel to the axis of the Slyne Basin, a new set of ENE–WSW-oriented faults formed during the Cretaceous, observed offsetting the upper 100–200 ms TWTT of the Upper Jurassic section and the Cretaceous section in the northern Slyne sub-basin (O'Sullivan and Childs, 2021).

A second period of uplift and erosion occurred during the early Cenozoic throughout the Slyne Basin, forming another regional unconformity (Figs. 4–8). This was accompanied by a period of regional magmatism, expressed as igneous intrusions observed throughout the Slyne Basin (Figs. 4, 6, 7, 8) and layers of basaltic lava in the northern and southern Slyne sub-basins (Figs. 4, 7).

Cenozoic tectonic activity reactivated several structures throughout the Slyne Basin with different expressions and senses of motion in different sub-basins. In the northern Slyne sub-basin the delamination fault above the Corrib anticline was reactivated for a second time, offsetting the early Eocene lavas of the Druid Formation, alongside the large listric fault to the west of Corrib (Fig. 7). In the central and southern Slyne sub-basins, several intra-basinal faults were reactivated, with both normal and reverse motion observed on faults with Cenozoic throw between 10 and 50 ms TWTT (Figs. 5, 12d). The large listric fault in the central Slyne sub-basin was inverted along with some of the rafted fault blocks along the eastern margin of the basin (Figs. 5, 12d). In the central Slyne sub-basin the bounding fault along the western margin of the basin was reactivated during the Cenozoic, with between 50–150 ms TWTT of throw recorded along its length (Figs. 5, 12a). The faults bounding the northern Slyne sub-basin were not reactivated during the Cenozoic (Figs. 6–8, 12a), but due to thermal subsidence in the neighbouring Rockall Basin, the Cenozoic sequence thickens significantly along the western margin of the northern Slyne sub-basin (Figs. 7, 8, 12a).

5 Discussion

5.1 Structural inheritance and the impact of oblique pre-existing structures

Structural inheritance is a common feature across the sedimentary basins of NW Europe, with Carboniferous, Permian, Jurassic, and Cretaceous rifting interpreted to reacti-vate older, pre-existing structures which formed during the Caledonian or Variscan orogenies. This is recorded along the Atlantic margin of NW Europe (Stein, 1988; Doré et al., 1999; Ziegler and Dèzes, 2006; Schiffer et al., 2019) as well as in the basins of the North Sea (Fazlikhani et al., 2017; Phillips et al., 2019; Osagiede et al., 2020). The reactivation of structures has been observed both onshore and offshore Ireland, with faults in the Carboniferous basins in the Irish midlands forming parallel to the NE–SW structures in the Caledonian basement (Worthington and Walsh, 2011; Kyne et al., 2019), while Variscan structures form the template for the later development of the Celtic Sea basins (Van Hoorn, 1987; Shannon, 1991; Rodriguez-Salgado et al., 2019, 2022). Similar relationships have been suggested for the Irish Atlantic margin (Tate and Dobson, 1989; Naylor and Shannon, 2005), with several Caledonian structures mapped onshore continuing into the offshore domain (Fig. 1).

The relationship between pre-existing basement structure and basin formation has been studied extensively from outcrop and subsurface mapping and using analogue modelling (e.g. Tommasi and Vauchez, 2001; Fazlikhani et al., 2017; Collanega et al., 2019). The key factor that determines the nature of this relationship is the relative orientation of inherited structure and the later extension direction (e.g. Henza et al., 2011; Henstra et al., 2015). Where inherited structures are at a low angle to the extension direction, they are not reactivated but may impede the propagation of new extensional faults and may give rise to transfer zones between adjacent fault and basin segments. As the angle between pre-existing structures and extension direction increases, the likelihood of reactivation of basement structure increases, and analogue modelling has demonstrated the variety of fault patterns that can form in the cover sequence. Although the effect of basement structure can manifest in many ways the two situations that have received most attention are extension oblique to an individual basement fault (Schlische et al., 2002) and oblique basin opening modelled by extension oblique to a zone of weakness (Agostini et al., 2009; Philipon and Corti, 2016). In both cases extension results in the formation of new fault segments or faults that are normal, or close to normal, to the extension direction and arranged en echelon above or within the basement structure or zone. Figure 13b illustrates fault and basin geometry that is characteristic of extension oblique to a basement fabric; the key feature is that the overall orientation of the basin is parallel to the basement structure, while individual faults may not align with these basement structures. The Slyne Basin does not follow Caledonian basement structure but cuts across it and as a result displays a different style of inheritance. Figures 13a and 14a illustrate our interpretation of the initial Jurassic geometry of the Slyne Basin that is based on observations below; this geometry resembles that in Fig. 13c in which individual fault segments follow the basement structures, but the basin as a whole cuts across it.

The Slyne Basin strikes NNE–SSW (020°) and cuts across the local Caledonian inherited trend oriented NE–SW (ca.
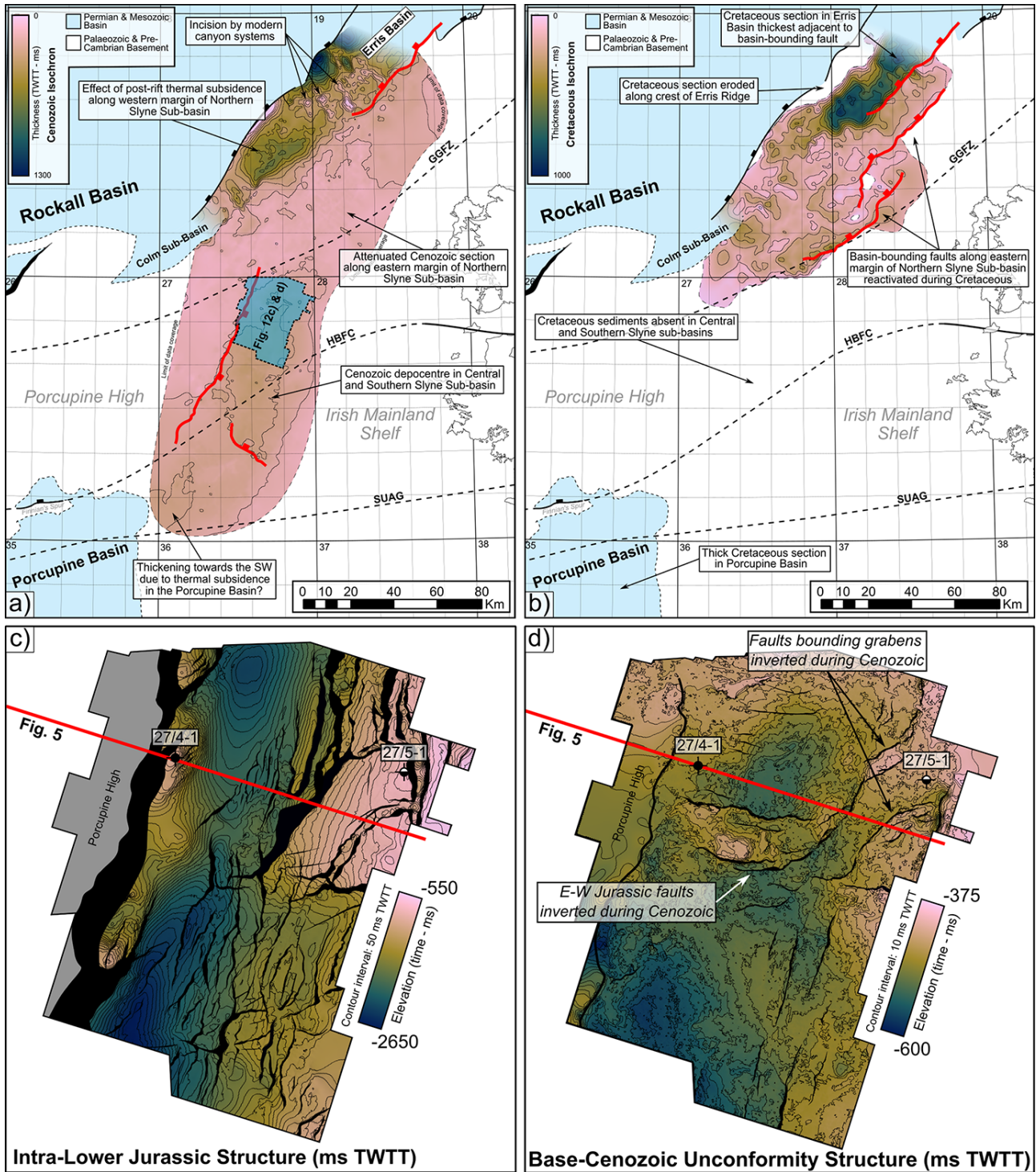
Figure 12. (a) TWTT thickness map (isochron) of the Cenozoic section in the Slyne and southern Erris basins superimposed on the syn-rift structural features. A thicker Cenozoic section is observed along the western margin of the northern Slyne sub-basin and in the southern Erris Basin. This is transected by modern slope canyons which incise into the Cenozoic section. A thicker Cenozoic section is also observed in the central Slyne sub-basin. **(b)** TWTT thickness map (isochron) for the Cretaceous section in the Slyne and southern Erris basins superimposed on the syn-rift structural features. Cretaceous strata are absent in the Slyne Basin south of the Central Slyne Transfer Zone but are present in the North Porcupine Basin. A significantly thicker Cretaceous section is preserved in the southern Erris Basin, although it is eroded along the north-western margin of the Erris Basin. **(c)** TWTT structure map of the intra-Lower Jurassic in the central Slyne Basin. **(d)** TWTT structure map of the Base Cenozoic Unconformity in the central Slyne sub-basin. Notice the subtle inversion structures, including a WNW–ESE block in the centre of the map and small grabens around the 27/5-1 well.

Table 1. Exhumation estimates from different locations throughout the Slyne Basin. Well locations are shown in Figs. 1 and 3.

Exhumation estimate (km)	Location	Source
0.7–1.9	27/13-1	Scotchman and Thomas (1995)
0.8–1.7	Corrib	Corcoran and Mecklenburgh (2005)
0.7–3.2	Central and southern Slyne sub-basins	Biancotto et al. (2007)
1.6–2.0	27/24-sb02	Fugro (1994b)
1.8	27/5-1	Geotrack (1996)
0.8–2.6	19/8-1	Geotrack (2008)

045°). On the eastern flank of the northern Slyne sub-basin the bounding faults parallel the Caledonian trend and form a left-stepping fault array (Fig. 1). The map pattern on the western flank is somewhat obscured by erosion and data quality, but the faults also parallel the Caledonian trend. Within the central Slyne Basin the faults offsetting the Jurassic are predominantly parallel to the basin axis (Fig. 11b). The majority of these faults are confined to the Jurassic section and are decoupled from the Carboniferous basement by the Zechstein salt (Fig. 5). The fault forming the western flank of the central Slyne Basin is approximately parallel to the basin trend (Fig. 1), but closer inspection (Fig. 11a) shows that it has a distinct splay in the sub-salt basement. This fault pattern is consistent with this margin of the basin originating as a left-stepping fault array that would have comprised fault segments parallel to the preserved splays, i.e. at a strike of ca. 040° and close to the orientation of the Caledonian basement fabric. We therefore suggest that the main faults that bound the Slyne Basin during Jurassic extension initially comprised left-stepping arrays of fault segments that individually followed the Caledonian NE–SW trend (Figs. 13a, 14). This initial segmentation is preserved in the fault array bounding the eastern margin of the northern Slyne sub-basin but was bypassed by the formation of a through-going, basin-parallel (i.e. NNE–SSW-oriented) fault in the central Slyne sub-basin. The reason for the different style of basin-bounding fault evolution observed either side of the GGFZ is difficult to assess with current data. Some potential reasons may be the change in orientation of Caledonian structures from NE–SW to E–W towards the south or the varying composition of the Lewisian and Dalradian basement located north and south of the GGFZ, respectively.

The Slyne Basin provides an example of a form of basement control that is not frequently documented in the literature. In general, individual faults are sub-perpendicular to the extension direction, whether they be segments of a fault located above a reactivated basement structure or faults within an oblique rift. The Slyne Basin cuts across the basement trend, but the individual basin-bounding faults follow the basement trend. These two styles of interaction are compared in Fig. 13b and c. A key difference between these is that there is a reversal of the sense of stepping of the basin-bounding faults despite the fact that the angular relationship between the basement and the extension direction is the same. This style of inheritance is not generally recognised in analogue modelling, but Corti et al. (2007) generated this pattern by introducing discrete narrow zones of weakness (Fig. 13d). Their model, designed to replicate the structure of the western branch of the East African Rift System, generated left-stepping rift-bounding faults in the presence of E–W extension by reactivation of discrete crustal structures in a pattern very similar to that seen in the Slyne Basin. While this style of inheritance is perhaps unusual, there are other areas in which it can be observed. In the northern North Sea, a Triassic–Jurassic broadly N–S rift system formed on crust with both N–S- and NE–SW-oriented Devonian and Caledonian crustal structures. The North Sea basins display a wide variety of styles of inheritance (Fazlikhani et al., 2017; Phillips et al., 2019), but a common feature is that major faults that parallel Caledonian trends are left-stepping, and the map pattern of the Viking Graben, for example, is similar to that of the East African Rift shown in Fig. 13d.

5.2 Post-rift uplift and erosion

A significant section of the syn-rift section is absent from the Slyne Basin, with key structural geometries recorded in the Upper Jurassic syn-rift sequences missing due to kilometre-scale uplift and erosion during the Cretaceous and Cenozoic (Table 1). The magnitude of uplift and erosion throughout the Slyne and Erris basins is highly variable. Previous authors have recorded a wide range of values for the magnitude of this post-rift exhumation, ranging from a few hundred metres to several kilometres (Scotchman and Thomas, 1995; Corcoran and Clayton, 2001; Doré et al., 2002; Corcoran and Mecklenburgh, 2005; Biancotto et al., 2007). This variability in exhumation estimates arises due to the geological complexity associated with this process; in the Slyne Basin, three discrete post-rift unconformities are observed: the Base Cretaceous, Base Cenozoic, and mid-Miocene unconformities. These unconformities are the result of a variety of both local and regional tectonic processes, including rift-shoulder uplift associated with rifting and hyperextension in the neighbouring Rockall Basin, the opening of the Bay of Biscay, the development of the Icelandic plume and the North Atlantic Igneous Province, ridge push at the Mid-Atlantic Ridge, the Alpine Orogeny, and possibly the development of
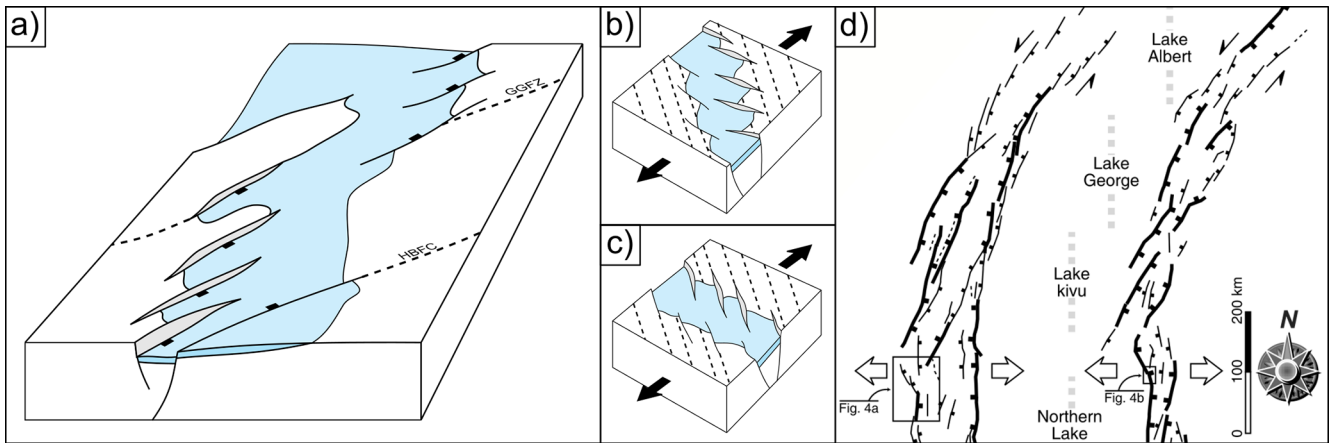
Figure 13. **(a)** Schematic block model showing the initial fault segments of the basin-bounding faults and the reversal in basin polarity across the GGFZ. **(b–c)** Block models showing different patterns of basement formation when extension is oblique to pre-existing structures. Dashed lines represent pre-existing structures, white polygons represent active faults, and blue polygons represent the actively forming rift basin. **(b)** Basin orientation matches pre-existing structures, while active faults crosscut them. **(c)** Active faults match pre-existing structures, while the basin crosscuts them **(d)** Section of Fig. 3 of Corti et al. (2007) demonstrating similar rift geometries to those observed in the Slyne Basin.
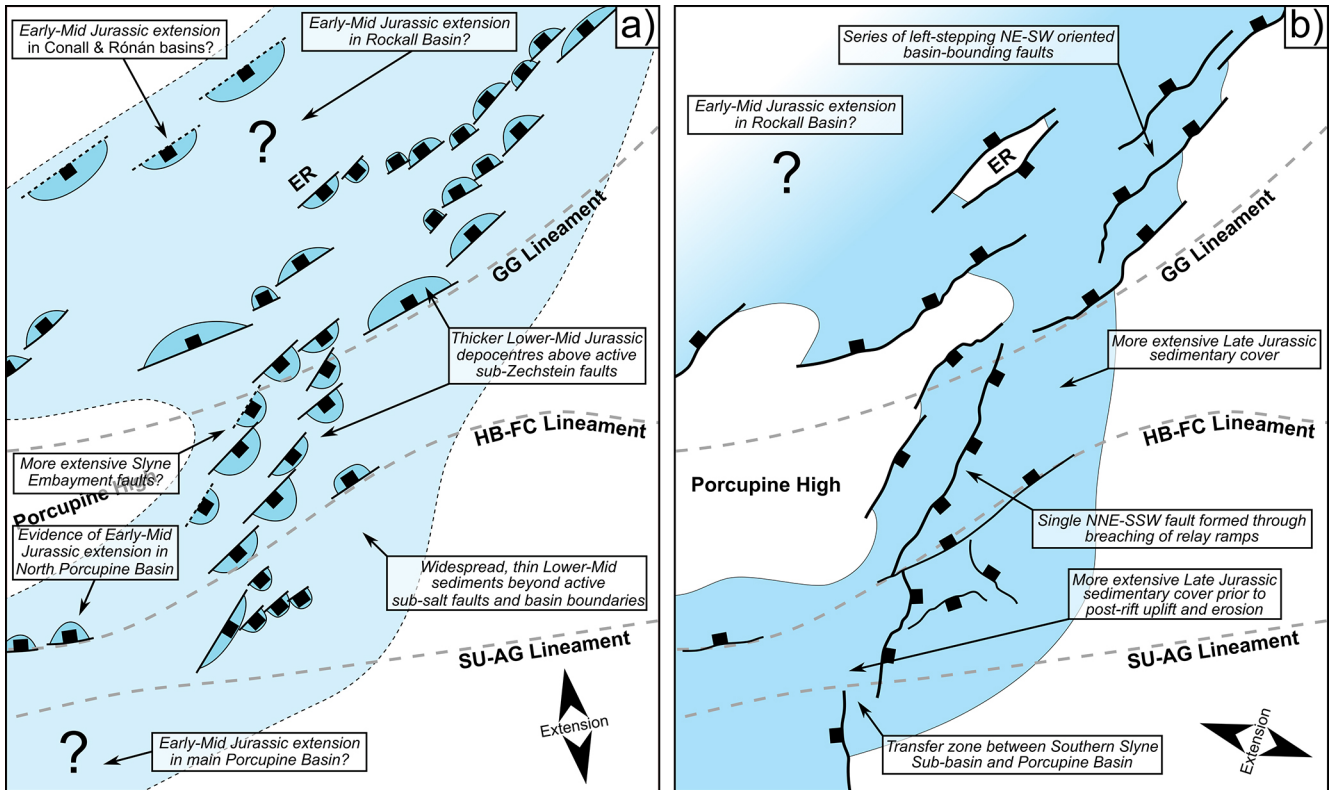
Figure 14. Conceptual maps showing the evolution of the main basin-bounding and intra-basinal faults in the Slyne Basin and surrounding areas during the **(a)** Early to Middle Jurassic and **(b)** Late Jurassic.

the Brendan Igneous Centre (Fig. 1; Mohr, 1982; Dancer et al., 1999). Additionally, these unconformities become composite surfaces at different locations within the Slyne Basin: the absence of Cretaceous strata in the central and southern Slyne sub-basins (Fig. 12b) may be due to non-deposition or, more likely, the erosion of the thin Cretaceous section, similar to that observed in the northern Slyne sub-basin, during the Cenozoic uplift events. The formation of these composite unconformities obscures the reactivation of any syn-rift faults in the central and southern Slyne sub-basins during the Cretaceous, as the circa 100–300 m of erosion at the Base Cenozoic Unconformity (sensu Corcoran and Mecklenburgh, 2005) is greater than the throw recorded on most of the Cretaceous faults observed in the northern Slyne sub-basin (Figs. 6, 7). Finally, the multitude of methodologies used to estimate exhumation varies throughout the basin and includes vitrinite reflectance (Scotchman and Thomas, 1995; Corcoran and Clayton, 2001), compaction analysis (Corcoran and Mecklenburgh, 2005), and analysis of seismic velocities (Biancotto et al., 2007).

A further consequence of this extensive and variable erosion during the Cretaceous and Cenozoic is that the present-day boundaries of the basin are not representative of their full extent during the Upper Jurassic syn-rift period. The Mesozoic rift basins on the Irish Atlantic margin, including the Slyne Basin, were much more extensive prior to uplift and erosion. Consequently, some publications have, as a result, focused on individual basins as separate and different geological entities rather than as residual parts of a complex, margin-wide rift system. Possible reconstructions of the Slyne Basin and neighbouring areas during the Early–Middle and Late Jurassic periods are presented in Fig. 14.

5.3 The Slyne Basin in the context of the Irish Atlantic margin

As stated above, the Slyne Basin belongs to a framework of basins which stretch across the Irish Atlantic margin and likely shares aspects of its geological evolution with these other areas. The most similar of these neighbours is the Erris Basin directly north of the northern Slyne sub-basin (Fig. 1). The Erris Basin is contiguous with and has a similar sedimentary fill to the Slyne Basin, which suggest that both basins underwent a similar geological evolution during the Permian, Triassic, and Jurassic periods (Fig. 8). The evolution of the Slyne and Erris basins diverges in the Cretaceous, with the thicker Cretaceous section in the Erris Basin (Figs. 8, 12b) indicating it underwent active extension during the Cretaceous alongside the neighbouring Rockall Basin, while the Slyne Basin remained largely inactive.

The Slyne Basin is separated from the Porcupine Basin by a narrow basement high approximately 5 km wide (Fig. 4). This high is the eroded footwall of the fault bounding the southern Slyne sub-basin, with kilometre-scale erosion largely taking place during the Cretaceous and Cenozoic

(Dancer et al., 1999; Biancotto et al., 2007). Restoring a kilometre-scale section of Upper Jurassic stratigraphy would connect the Porcupine Basin with the southern Slyne sub-basin, supporting the idea that these basins developed co-evally during the Late Jurassic (Fig. 14b). The nearby 26/30-1 well in the Porcupine Basin (Fig. 4) encountered the Upper Jurassic Minard Formation resting unconformably atop the Carboniferous Blackthorn Group (Phillips Petroleum Company, 1982), while the intervening Permian to Middle Jurassic stratigraphy present in the southern Slyne sub-basin is absent. While Triassic and Lower Jurassic stratigraphy has been encountered in two wells in the North Porcupine Basin to the north of Finnian's Spur (Fig. 1b; Bulois et al., 2018; Merlin Energy Resources Consortium, 2020), most wells in the North Porcupine Basin encountered Upper Jurassic sediments resting directly atop Carboniferous sediments (Merlin Energy Resources Consortium, 2020). Permian sediments have not been encountered in any well in the Porcupine Basin (Merlin Energy Resources Consortium, 2020). This indicates that the Slyne Basin is the older of the two basins, with extension beginning in the Late Permian with the deposition of several 100 m of Zechstein Group evaporites (Štolfová and Shannon, 2009; O'Sullivan et al., 2021), while the North Porcupine Basin likely remained a relative high during the latest Palaeozoic and early Mesozoic. There may be narrow outliers of Permian, Triassic, and Early to Middle Jurassic-aged sediments preserved beneath the Late Jurassic sediments further south in the Porcupine Basin, but at present this remains unproven.

6 Conclusions

Detailed interpretation of available seismic reflection data in conjunction with borehole and potential-field datasets has delivered an improved understanding of the complex and multiphase structural history of the Slyne Basin.

The onset of rifting in the Slyne Basin began in the Late Permian, expressed as diffuse extensional faulting accompanied by the deposition of the Zechstein Group evaporites in localised, fault-bounded depocentres. This was followed by tectonic quiescence during the majority of the Triassic and subsequent extension accompanied by halokinesis during the Latest Triassic and into the Early and Middle Jurassic. Regional uplift and erosion occurred during the late Middle Jurassic, creating a regional unconformity. The main phase of rifting began in the Oxfordian and continued until the end of the Jurassic, with the basin-bounding faults accumulating several kilometres of slip during this time.

The Slyne Basin experienced kilometre-scale uplift and erosion throughout the Early Cretaceous, creating the distinct angular unconformity between Jurassic syn-rift sediments and Cretaceous and younger post-rift sediments. Subsequent and less severe phases of exhumation occurred during the Cenozoic. Faults throughout the basin are reactivated

in both normal and reverse senses during this tectonic activity.

Salt layers in the Slyne Basin exert important controls on basin development, most importantly acting as décollements between the Palaeozoic pre-salt basement and Mesozoic post-salt basin fill. The most important salt-prone interval is the Permian Zechstein Group, present throughout the Slyne Basin, while in the northern sub-basin the Upper Triassic Uilleann Halite Member is also present, acting as a second layer of mechanical detachment.

The segmentation of the Slyne Basin into discrete sub-basins occurs where crustal-scale structural lineaments, representing the suture zones and boundaries between Caledonian and Precambrian terranes, obliquely transect the younger Mesozoic basin.

The basin axis is oriented NNE–SSW and cuts across the N–E Caledonian trend, resulting in a rarely documented style of fault reactivation in which the segments of basin-bounding faults follow the earlier structural grain but the basin as a whole does not. As strain increased, initial left-stepping segments linked, resulting in basin-bounding faults oriented parallel to the basin axis.

References

Ady, B. E. and Whittaker, R. C.: Examining the influence of tectonic inheritance on the evolution of the North Atlantic using a palinspastic deformable plate reconstruction, Geol. Soc. Lond. Spec. Publ., 470, 245–264, https://doi.org/10.1144/SP470.9, 2019.

Agostini, A., Corti, G., Zeoli, A., and Mulugeta, G.: Evolution, pattern, and partitioning of deformation during oblique continental rifting: Inferences from lithospheric-scale centrifuge models, Geochem. Geophy. Geosy., 10, Q11015, https://doi.org/10.1029/2009GC002676, 2009.

Alves, T. M., Moita, C., Sandnes, F., Cunha, T., Monteiro, J. H., and Pinheiro, L. M.: Mesozoic-Cenozoic evolution of North Atlantic continental-slope basins: The Peniche basin, western Iberian margin, AAPG Bull., 90, 31–60, https://doi.org/10.1306/08110504138, 2006.

Anderson, H., Walsh, J. J., and Cooper, M. R.: The development of a regional-scale intraplate strike-slip fault system; Alpine deformation in the north of Ireland, J. Struct. Geol., 116, 47–63, 2018.

Badley, M.: Late Tertiary faulting, footwall uplift and topography in western Ireland, Geol. Soc. Lond. Spec. Publ., 188, 201–207, https://doi.org/10.1144/GSL.SP.2001.188.01.11, 2001.

Biancotto, F., Hardy, R. J. J., Jones, S. M., Brennan, D., and White, N. J.: Estimating denudation from seismic velocities offshore northwest Ireland, in: SEG Technical Program Expanded Abstracts 2007, 407–411, https://doi.org/10.1190/1.2792452, 2007.

Bird, P. C., Cartwright, J. A., and Davies, T. L.: Basement reactivation in the development of rift basins: an example of reactivated Caledonide structures in the West Orkney Basin, J. Geol. Soc., 172, 77–85, 2014.

Brown, A. R.: Calibrate yourself to your data! A vital first step in seismic interpretation, Geophys. Prospect., 49, 729–733, 2001.

Bulois, C., Pubellier, M., Chamot-Rooke, N., and Watremez, L.: From orogenic collapse to rifting: A case study of the northern Porcupine Basin, offshore Ireland, J. Struct. Geol., 114, 139–162, https://doi.org/10.1016/j.jsg.2018.06.021, 2018.

Chapman, T. J., Broks, T. M., Corcoran, D. V., Duncan, L. A., and Dancer, P. N.: The structural evolution of the Erris Trough, offshore northwest Ireland, and implications for hydrocarbon generation, Geological Society, London, Petroleum Geology Conference Series, 5, 455–469, https://doi.org/10.1144/0050455, 1999.

Collanega, L., Siuda, K., Jackson, C. A.-L., Bell, R. E., Coleman, A. J., Lenhart, A., Magee, C., and Breda, A.: Normal fault growth influenced by basement fabrics: The importance of preferential nucleation from pre-existing structures, Basin Res., 31, 659–687, https://doi.org/10.1111/bre.12327, 2019.

Corcoran, D. V. and Clayton, G.: Interpretation of vitrinite reflectance profiles in sedimentary basins, onshore and offshore Ireland, Geol. Soc. Lond. Spec. Publ., 188, 61–90, https://doi.org/10.1144/GSL.SP.2001.188.01.04, 2001.

Corcoran, D. V. and Doré, A. G.: Depressurization of hydrocarbon-bearing reservoirs in exhumed basin settings: evidence from Atlantic margin and borderland basins, Geol. Soc. Lond. Spec. Publ., 196, 457–483, https://doi.org/10.1144/GSL.SP.2002.196.01.25, 2002.

Corcoran, D. V. and Mecklenburgh, R.: Exhumation of the Corrib Gas Field, Slyne Basin, offshore Ireland, Petrol. Geosci., 11, 239–256, 2005.

Corfield, S., Murphy, N., and Parker, S.: The structural and stratigraphic framework of the Irish Rockall Trough, Petrol. Geol. Conf. P., 5, 407–420, https://doi.org/10.1144/0050407, 1999.

Corti, G., van Wijk, J., Cloetingh, S., and Morley, C. K.: Tectonic inheritance and continental rift architecture: Numerical and analogue models of the East African Rift system, Tectonics, 26, TC6006, https://doi.org/10.1029/2006TC002086, 2007.

Cunningham, G. A. and Shannon, P. M.: The Erris Ridge: A major geological feature in the NW Irish Offshore Basins, J. Geol. Soc., 154, 503–508, 1997.

Dancer, P. N. and Pillar, N. W.: Exploring in the Slyne Basin: a geophysical challenge, The Petroleum Exploration of Ireland's Offshore Basins, 188, 209–222, 2001.

Dancer, P. N., Algar, S. T., and Wilson, I. R.: Structural evolution of the Slyne Trough, Petroleum Geology of Northwest Europe: Proceedings of the 5th Conference on the Petroleum Geology of Northwest Europe, 1, 445–454, 1999.

Dancer, P. N., Kenyon-Roberts, S. M., Downey, J. W., Baillie, J. M., Meadows, N. S., and Maguire, K.: The Corrib gas field, offshore west of Ireland, Geological Society, London, Petroleum Geology Conference series, 6, 1035–1046, 2005.

Doré, A. G., Lundin, E. R., Jensen, L. N., Birkeland, O., Eliassen, P. E., and Fichler, C.: Principal tectonic events in the evolution of the northwest European Atlantic margin, Petroleum Geology of Northwest Europe: Proceedings of the 5th Conference, 41–61, 1999.

Doré, A. G., Corcoran, D. V., and Scotchman, I. C.: Prediction of the hydrocarbon system in exhumed basins, and application to the NW European margin, Geol. Soc. Spec. Publ., 196, 401–429, https://doi.org/10.1144/GSL.SP.2002.196.01.21, 2002.

Doré, A. G., Lundin, E. R., Fichler, C., and Olesen, O.: Patterns of basement structure and reactivation along the NE Atlantic margin, J. Geol. Soc., 154, 85–89, 2007.

Droujinine, A., Buckner, S., and Cameron, R.: Full-wave long offset seismic imaging and velocity analysis with gravity and well constraints – a case study from NW Corrib, offshore Ireland, in: SEG Technical Program Expanded Abstracts 2005, Society of Exploration Geophysicists, 409–412, 2005.

Fazlikhani, H., Fossen, H., Gawthorpe, R. L., Faleide, J. I., and Bell, R. E.: Basement structure and its influence on the structural configuration of the northern North Sea rift, Tectonics, 36, 1151–1177, https://doi.org/10.1002/2017TC004514, 2017.

Fugro: Field Report Irish Frontier Shallow Coring Project Blocks 19/13 and 27/24 Irish Sector Atlantic Ocean (Volume I), 1994a.

Fugro: Field Report Irish Frontier Shallow Coring Project Blocks 19/13 and 27/24 Irish Sector Atlantic Ocean (Volume II), 1994b.

Gawthorpe, R. L. and Hurst, J. M.: Transfer zones in extensional basins: their structural style and influence on drainage development and stratigraphy, J. Geol. Soc., 150, 1137–1152, 1993.

Geotrack: Thermal history reconstruction in well 27/5-1 west of Ireland using apatite fission track analysis and vitrinite reflectance, Report compiled by: Gibson, H. J., 1996.

Geotrack: Thermal history reconstruction in offshore Ireland well 19/8-1, based on AFTA® and VR data, Report compiled by: Green, P. F., 2008.

Hardy, R. J. J., Querendez, E., Biancotto, F., Jones, S. M., O'Sullivan, J., and White, N.: New methods of improving seismic data to aid understanding of passive margin evolution: a series of case histories from offshore west of Ireland, Petroleum Geology: From Mature Basins to New Frontiers – Proceedings of the 7th Petroleum Geology Conference, 7, 1005–1012, 2010.

Henstra, G. A., Rotevatn, A., Gawthorpe, R. L., and Ravnås, R.: Evolution of a major segmented normal fault during multiphase rifting: The origin of plan-view zigzag geometry, J. Struct. Geol., 74, 45–63, 2015.

Henza, A. A., Withjack, M. O., and Schlische, R. W.: How do the properties of a pre-existing normal-fault population influence fault development during a subsequent phase of extension?, J. Struct. Geol., 33, 1312–1324, 2011.

Jones, D. W. and Underhill, J. R.: Structural and stratigraphic evolution of the Connemara discovery, Northern Porcupine Basin: significance for basin development and petroleum prospectivity along the Irish Atlantic Margin, Petrol. Geosci., 17, 365–384, https://doi.org/10.1144/1354-079310-035, 2011.

Kimbell, G. S., Ritchie, J. D., and Henderson, A. F.: Three-dimensional gravity and magnetic modelling of the Irish sector of the NE Atlantic margin, Tectonophysics, 486, 36–54, https://doi.org/10.1016/j.tecto.2010.02.007, 2010.

Klemperer, S. L., Ryan, P. D., and Snyder, D. B.: A deep seismic reflection transect across the Irish Caledonides, J. Geol. Soc., 148, 149–164, https://doi.org/10.1144/gsjgs.148.1.0149, 1991.

Kyne, R., Torremans, K., Güven, J., Doyle, R., and Walsh, J.: 3-D modeling of the lisheen and silvermines deposits, County Tipperary, Ireland: insights into structural controls on the formation of Irish Zn-Pb deposits, Econ. Geol., 114, 93–116, https://doi.org/10.5382/econgeo.2019.4621, 2019.

Lefort, J. P. and Max, M. D.: Development of the Porcupine Seabight: use of magnetic data to show the direct relationship between early oceanic and continental structures, J. Geol. Soc., 141, 663–674, https://doi.org/10.1144/gsjgs.141.4.0663, 1984.

Merlin Energy Resources Consortium: The Standard Stratigraphic Nomenclature of Offshore Ireland: An Integrated Lithostrati-

graphic, Biostratigraphic and Sequence Stratigraphic Framework, Project Atlas, Petroleum Affairs Division, Department of the Environment, Climate and Communications, Special Publication 1/21, 2020.

Mohr, P.: Tertiary dolerite intrusions of west-central Ireland, Proceedings Royal Irish Academy, 82B, 53–82, 1982.

Morley, C. K., Nelson, R. A., Patton, T. L., and Munn, S. G.: Transfer Zones in the East African Rift System and Their Relavance to Hydrocarbon Exploration in Rifts, American Association of Petroleum Geologists Bulletin, 74, 1234–1253, 1990.

Morley, C. K., Haranya, C., Phoosongsee, W., Pongwapee, S., Kornsawan, A., and Wonganan, N.: Activation of rift oblique and rift parallel pre-existing fabrics during extension and their effect on deformation style: examples from the rifts of Thailand, J. Struct. Geol., 26, 1803–1829, 2004.

Musgrove, F. W. and Mitchener, B.: Analysis of the pre-tertiary rifting history of the Rockall Trough, Petroleum Geoscience, 2, 353–360, https://doi.org/10.1144/petgeo.2.4.353, 1996.

Naylor, D. and Shannon, P. M.: The structural framework of the Irish Atlantic Margin, Geological Society, London, Petroleum Geology Conference series, 6, 1009–1021, https://doi.org/10.1144/0061009, 2005.

Naylor, D., Shannon, P., and Murphy, N.: Irish Rockall Basin Region – a standard structural nomenclature system, Petroleum Affairs Division, Special Publication 1/99, 1999.

Osagiede, E. E., Rotevatn, A., Gawthorpe, R., Kristensen, T. B., Jackson, C. A. L., and Marsh, N.: Pre-existing intra-basement shear zones influence growth and geometry of non-colinear normal faults, western Utsira High–Heimdal Terrace, North Sea, J. Struct. Geol., 130, 103908, https://doi.org/10.1016/j.jsg.2019.103908, 2020.

O'Sullivan, C. and Childs, C.: Kinematic interaction between stratigraphically discrete salt layers; the structural evolution of the Corrib gas field, offshore NW Ireland, Mar. Petrol. Geol., 133, 105274, https://doi.org/10.1016/j.marpetgeo.2021.105274, 2021.

O'Sullivan, C. M., Childs, C. J., Saqab, M. M., Walsh, J. J., and Shannon, P. M.: The influence of multiple salt layers on rift-basin development; The Slyne and Erris basins, offshore NW Ireland, Basin Res., 33, 2018–2048, https://doi.org/10.1111/bre.12546, 2021.

PAD: Search Petroleum Exploration and Production Data, Department of the Environment, Climate and Communications, Petroleum Affairs Division (PAD) [data set], https://www.gov.ie/en/service/search-petroleum-exploration-and-production-data/, last access: 23 October 2022.

Pereira, R. and Alves, T. M.: Margin segmentation prior to continental break-up: A seismic-stratigraphic record of multiphased rifting in the North Atlantic (Southwest Iberia), Tectonophysics, 505, 17–34, https://doi.org/10.1016/j.tecto.2011.03.011, 2011.

Pereira, R. and Alves, T. M.: Crustal deformation and submarine canyon incision in a Meso-Cenozoic first-order transfer zone (SW Iberia, North Atlantic Ocean), Tectonophysics, 601, 148–162, https://doi.org/10.1016/j.tecto.2013.05.007, 2013.

Pereira, R., Alves, T. M., and Mata, J.: Alternating crustal architecture in West Iberia: A review of its significance in the context of NE Atlantic rifting, J. Geol. Soc., 174, 522–540, https://doi.org/10.1144/jgs2016-050, 2017.

Philippon, M. and Corti, G.: Obliquity along plate boundaries, Tectonophysics, 693, 171–182, 2016.

Phillips Petroleum Company: Phillips Petroleum Company Ireland 26/30-1 Final Well Report, 1982.

Phillips, T. B., Jackson, C. A.-L., Bell, R. E., and Duffy, O. B.: Oblique reactivation of lithosphere-scale lineaments controls rift physiography – the upper-crustal expression of the Sorgenfrei–Tornquist Zone, offshore southern Norway, Solid Earth, 9, 403–429, https://doi.org/10.5194/se-9-403-2018, 2018.

Phillips, T. B., Fazlikhani, H., Gawthorpe, R. L., Fossen, H., Jackson, C. A. L., Bell, R. E., Faleide, J. I., and Rotevatn, A.: The Influence of Structural Inheritance and Multiphase Extension on Rift Development, the Northern North Sea, Tectonics, 38, 4099–4126, https://doi.org/10.1029/2019TC005756, 2019.

Roberts, D., Thompson, M., Mitchener, B., Hossack, J., Carmicheal, S., and Bjornseth, H.-M.: Palaeozoic to Tertiary rift and basin dynamics: mid-Norway to the Bay of Biscay – a new context for hydrocarbon prospectivity in the deep water frontier, Geological Society, London, Petroleum Geology Conference series, 5, 7–40, https://doi.org/10.1144/0050007, 1999.

Robeson, D., Burnett, R. D., and Clayton, G.: The Upper Palaeozoic Geology of the Porcupine, Erris and Donegal Basins, Offshore Ireland, Irish J. Earth Sci., 9, 153–175, 1988.

Rodríguez-Salgado, P., Childs, C., Shannon, P. M., and Walsh, J. J.: Structural evolution and the partitioning of deformation during basin growth and inversion: A case study from the Mizen Basin Celtic Sea, offshore Ireland, Basin Res., 32, 830–853, https://doi.org/10.1111/bre.12402, 2019.

Rodríguez-Salgado, P., Childs, C., Shannon, P. M., and Walsh, J. J.: The influence of basement fabrics on fault reactivation during rifting and inversion; a case study from the Celtic Sea basins, offshore Ireland, J. Geol. Soc., 13, 315–338, https://doi.org/10.1144/jgs2022-024, 2022.

Rohrman, M.: Prospectivity of volcanic basins: Trap delineation and acreage de-risking, AAPG Bull., 91, 915–939, 2007.

Saqab, M. M., Childs, C., Walsh, J., Delogkos, E.: Multiphase deformation history of the Porcupine Basin, offshore west Ireland, Basin Res., 33, 1776–1797, https://doi.org/10.1111/bre.12535, 2020.

Schiffer, C., Doré, A. G., Foulger, G. R., Franke, D., Geoffroy, L., Gernigon, L., Holdsworth, R. E., Kusznir, N., Lundin, E., McCaffrey, K., Peace, A. L., Petersen, K. D., Phillips, T. B., Stephenson, R., Stoker, M. S., and Welford, J. K.: Structural inheritance in the North Atlantic, Earth-Sci. Rev., 206, 102975, https://doi.org/10.1016/j.earscirev.2019.102975, 2019.

Schlische, R. W., Withjack, M. O., and Eisenstadt, G.: An experimental study of the secondary deformation produced by oblique-slip normal faulting, AAPG Bull., 86, 885–906, 2002.

Schumacher, M. E.: Upper Rhine Graben: Role of preexisting structures during rift evolution, Tectonics, 21, 6-1–6-17, https://doi.org/10.1029/2001TC900022, 2002.

Scotchman, I. C. and Thomas, J. R. W.: Maturity and hydrocarbon generation in the Slyne Trough, northwest Ireland, The Petroleum Geology of Ireland's Offshore Basins, 93, 385–412, 1995.

Shannon, P. M.: The development of Irish offshore sedimentary basins, J. Geol. Soc., 148, 181–189, 1991.

Shannon, P. M.: Old challenges, new developments and new plays in Irish offshore exploration, Geological Society, London, Petroleum Geology Conference series, 8, 171–185, https://doi.org/10.1144/PGC8.12, 2018.

Stein, A. M.: Basement controls upon basin development in the Caledonian foreland, NW Scotland, Basin Res., 1, 107–119, https://doi.org/10.1111/j.1365-2117.1988.tb00008.x, 1988.

Štolfová, K. and Shannon, P. M.: Permo-Triassic development from Ireland to Norway: basin architecture and regional controls, Geol. J., 44, 652–676, 2009.

Tate, M. P.: The Clare Lineament: A relic transform fault west of Ireland, Geol. Soc. Spec. Publ., 62, 375–384, https://doi.org/10.1144/GSL.SP.1992.062.01.28, 1992.

Tate, M. P. and Dobson, M. R.: Late Permian to early Mesozoic rifting and sedimentation offshore NW Ireland, Mar. Petrol. Geol., 6, 49–59, https://doi.org/10.1016/0264-8172(89)90075-5, 1989.

Tommasi, A. and Vauchez, A.: Continental rifting parallel to ancient collisional belts: An effect of the mechanical anisotropy of the lithospheric mantle, Earth Planet. Sc. Lett., 185, 199–210, https://doi.org/10.1016/S0012-821X(00)00350-2, 2001.

Trueblood, S. and Morton, N.: Comparative Sequence Stratigraphy and Structural Styles of the Slyne Trough and Hebrides Basin, J. Geol. Soc., 148, 197–201, 1991.

Tyrrell, S., Haughton, P. D. W., and Daly, J. S.: Drainage reorganization during breakup of Pangea revealed by in-situ Pb isotopic analysis of detrital K-feldspar, Geology, 35, 971–974, https://doi.org/10.1130/G4123A.1, 2007.

Underhill, J. R. and Partington, M. A.: Jurassic thermal doming and deflation in the North Sea: Implications of the sequence stratigraphic evidence, Petrol. Geol. Conf. P., 4, 337–345, https://doi.org/10.1144/0040337, 1993.

Van Hoorn, B.: The south Celtic Sea/Bristol Channel Basin: origin, deformation and inversion history, Tectonophysics, 137, 309–317, 323, 326, 329–334, https://doi.org/10.1016/0040-1951(87)90325-8, 1987.

Vendeville, B. C. and Jackson, M. P. A.: The fall of diapirs during thin-skinned extension, Mar. Petrol. Geol., 9, 354–371, https://doi.org/10.1016/0264-8172(92)90048-J, 1992.

Walsh, A., Knag, G., Morris, M., Quinquis, H., Tricker, P., Bird, C., and Bower, S.: Petroleum geology of the Irish Rockall Trough – a frontier challenge, Geological Society, London, Petroleum Geology Conference Series, 5, 433–444, https://doi.org/10.1144/0050433, 1999.

Wilson, R. W., Holdsworth, R. E., Wild, L. E., Mccaffrey, K. J. W., England, R. W., Imber, J., and Strachan, R. A.: Basement-influenced rifting and basin development: A reappraisal of post-Caledonian faulting patterns from the North Coast Transfer Zone, Scotland, Geol. Soc. Spec. Publ., 335, 795–826, https://doi.org/10.1144/SP335.32, 2010.

Worthington, R. P. and Walsh, J. J.: Structure of Lower Carboniferous basins of NW Ireland, and its implications for structural inheritance and Cenozoic faulting, J. Struct. Geol., 33, 1285–1299, 2011.

Ziegler, P. A. and Dèzes, P.: Crustal evolution of Western and Central Europe, Geol. Soc. Lond. Mem., 32, 43–56, 2006.